

J. Kleperis · G. Wójcik · A. Czerwinski · J. Skowronski  
M. Kopczyk · M. Beltowska-Brzezinska

## Electrochemical behavior of metal hydrides

Received: 3 April 2000 / Accepted: 16 May 2000 / Published online: 13 March 2001  
© Springer-Verlag 2001

**Abstract** Metal hydride electrodes are of particular interest owing to their potential and practical application in batteries. A large number of hydrogen storage materials has been characterized so far. This paper deals with the effect of the chemical nature and stoichiometry of specific alloy families ( $AB_3$ ,  $A_2B$ ,  $AB/AB_2$  and  $AB_2$ ) on the hydride stability, hydrogen storage capacity and kinetics of hydrogen sorption-desorption in the solid phase/gas and solid phase/electrolyte solution systems. Special attention has been paid towards the electrochemical properties of metal hydrides in terms of their performance in Ni-MH rechargeable alkaline cells.

**Key words** Hydrogen absorption · Hydrogen storage alloys · Metal hydride electrodes · Nickel-metal hydride batteries

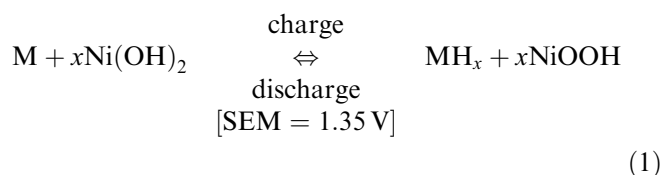
### Introduction

In the future, electrochemical energy storage and conversion systems will become increasingly important

owing to the rapid development of portable electronic devices, increasing concern about the environment and exhaustion of fossil fuel resources. Interest in metal hydrides as new negative electrode materials applicable in rechargeable nickel-metal hydride (Ni-MH) batteries has been growing since the 1960s.

During recent years there has been an increasing need to replace the toxic cadmium electrodes in Ni-Cd batteries by metal/metal hydride (M/MH) couples, relatively safe for the environment. Actually, Ni-MH batteries with the  $NiOOH/Ni(OH)_2$  positive electrode and M/MH negative electrode are considered as an alternative power source for electric vehicles (EV) which are being developed all around the world. The attractive features of Ni-MH batteries are the capability of high-rate charge-discharge, superior tolerance to overcharge-overdischarge and higher energy density in comparison with conventional lead-acid or nickel-cadmium systems (see Table 1).

The overall charge-discharge reaction in a Ni-MH battery is as follows:



On charging, the metal hydride (MH) is formed in the anode material (M), while the  $Ni(OH)_2$  at the cathode is transformed to nickel oxyhydroxide,  $NiOOH$ . The stored hydrogen is oxidized and the reduction of  $NiOOH$  occurs on discharging.

The M/MH electrode should be capable of reversible storing of hydrogen and should also exhibit an insignificant self-discharge. Since the reversibility of the charge-discharge reactions is required, a moderately stable hydride bonding between hydrogen and metal is desired. It is undesirable for the Me-H bond to be highly stable or very unstable. Because of this, detailed information about the energetics and kinetics of hydrogen

J. Kleperis (✉)  
University of Latvia, Institute of Solid State Physics,  
Kengaraga iela 8, 1063 Riga, Latvia  
E-mail: kleperis@latnet.lv  
Fax: +371-7112583

G. Wójcik · J. Skowronski · M. Kopczyk  
Central Laboratory of Cells and Batteries,  
Forteczna 12/14, 61-362 Poznan, Poland

A. Czerwinski  
Warsaw University, Department of Chemistry,  
Pasteura 1, 02-093 Warsaw, Poland

A. Czerwinski  
Industrial Chemistry Research Institute,  
Rydygiera 8, 01-793 Warsaw, Poland

J. Skowronski  
Poznan University of Technology, Piotrowo 3,  
60-965 Poznan, Poland

M. Beltowska-Brzezinska  
A. Mickiewicz University,  
Faculty of Chemistry Grunwaldzka 6, 60-780 Poznan, Poland

**Table 1** Rechargeable batteries selected for application in electric vehicles {ITE Battery Newslett (1997, 1998) and [6, 14]}

Technology	Environmental	Nominal voltage (V)	Costs (\$/Wh)	Specific energy (Wh/kg)	Cycle life
Lead-acid	Toxic	2.0	0.1–0.3	20–35	100–500
Ni-Metal hydride	Low toxicity	1.2	1.0–3.0	55–70	500
Ni-cadmium	Toxic	1.2	0.5–1.5	30–50	1000
Sodium-sulfur ( $T > 300$ °C)	Hazardous	2.0	–	170	1000
Zinc-air	Nontoxic	1.5	0.15–0.50	70–85	600
Lithium-ion	Hazardous	1.5–3.9	–	115–150	200–500

transfer processes occurring on/in electrode materials, as well as the specific energy, charge-discharge efficiency and cyclic lifetime of metal-hydride electrodes, are of a great importance for their future use in commercial batteries.

A large number of the hydrogen storage materials has been characterized so far. Their performance differs greatly in terms of charge and discharge behavior, self-discharge and cyclic lifetime. The first review on metal hydrides was written by Willems in 1984 [1]; the next one published in 1991 [2] gathered the articles that had been written since 1985. Presently, a number of reviews are available on this topic [1, 2, 3, 4, 5, 6, 7, 8, 9, 10, 11, 12, 13, 14, 15, 16]. These reviews deal mostly with specific alloy families, such as rare earth-nickel based systems and zirconium-titanium-vanadium-nickel Laves phase systems ( $AB_5$ ,  $AB_2$ , etc.), alloy preparation methods, discussion of thermodynamic and/or crystallographic data, as well as charge-discharge characteristics and some specific applications of the alloy electrodes in small sealed Ni-MH cells or batteries for electric vehicles. Recently, fullerene-based hydrides [17] with a specific capacity about 6–10 times larger than any metal hydride (but with a very poor cycling stability, so far) have been studied, focusing on their application for batteries. In this paper we have presented a comprehensive picture of the up-to-date knowledge about the properties of alloy materials of importance for their performance in hydrogen storage electrodes.

### Alloys and composition

The electrode materials used for hydrogen electrosorption were initially Pd, Pd/Ag, Raney nickel,  $LaNi_5$  and  $TiNi$  [18, 19, 20, 21, 22, 23, 24, 25]. These materials differ substantially from the ones used today. For example, Jung and Kroeger [25] describe a special type of Raney nickel (mixed with a thermoplastic synthetic resin) with a very large active surface and electrochemical capability to incorporate about 1.2 hydrogen atoms for every atom of metal. The field of Ni-MH secondary cells has grown rapidly in the past 15 years. Patents issued in the period 1988–1992 have been reviewed by Kleperis [16]. Special attention has been paid to palladium, which rapidly absorbs and desorbs large amounts of hydrogen. However, high cost was the main reason for the limited practical application of the Pd/PdH system. Thus

extensive efforts were taken to search for less expensive materials susceptible to hydrogen accommodation in their lattice. As a result of independent investigations performed in several laboratories, a wide set of alloys composed of rare earth elements with nickel ( $AB_5$ -type system) and alloys of zirconium, vanadium and/or titanium with nickel ( $A_2B$ -,  $AB$ - or  $AB_2$ -type systems) was offered for use as hydrogen storage materials. In these alloys, component A is the one which forms the stable hydride. Component B performs several additional functions: (1) it can play a catalytic role in enhancing the hydriding-dehydriding kinetic characteristics, (2) it can alter the equilibrium pressure of the hydrogen absorption-desorption process to desired level, (3) it can also increase the stability of the alloy, preventing dissolution or formation of a compact oxide layer of component A [3, 4, 5, 6, 7, 15].

### $AB_5$ -type alloys

The main example of the  $AB_5$  class alloy is  $LaNi_5$  with a hexagonal,  $CaCu_5$ -type structure containing three octahedral and three tetragonal sites per elemental cell unit [26].  $LaNi_5$  forms two hydrides, one with low hydrogen content ( $\alpha$  phase,  $LaNi_5H_{0.3}$ ) and the other with high hydrogen content ( $\beta$  phase,  $LaNi_5H_{5.5}$ ), which differ from each other significantly (about 25%) in the specific lattice volume. The discrete lattice expansion during conversion from the hydrogen solution phase ( $\alpha$ ) to the hydride phase ( $\beta$ ) promotes crumbling of the alloy particles on hydriding-dehydriding cycles.

An alloy of rare earth elements with nickel,  $MmNi_5$ , as the electrode in a fuel cell was used for the first time by Lindholm [22] in 1966 and then by Dilworth and Wunderlin [27, 28] in 1968. The term Mm (mischmetal) represents a natural mixture of rare earth elements, mostly consisting of Ce (30–52 wt%), La (13–25 wt%), Nd, Pr or Sm (13–57 wt%), with amounts depending on the place of origin [5]<sup>1</sup>. The  $LaNi_5$ -based electrode was first used in the low-pressure nickel-hydrogen cell by Dunlop and Stockel [29] in 1974.

In the  $AB_5$ -type alloy, both La and Ni can be replaced by other elements (Mm, Ce, Pr, Nd, Zr,

<sup>1</sup>The cost of Mm is much lower than that for La. The largest mischmetal supplier is China

Hf→La and Al, Mn, Si, Zn, Cr, Fe, Cu, Co→Ni), thereby altering the hydrogen storage capacity, the stability of the hydride phase or the corrosion resistance, etc. (see Table 2). Furthermore, a partial replacement of the A and B components significantly changes the alloy macrostructure, e.g. Mn facilitates nucleation [5]. Also, as reported by Notten et al. [30], the stoichiometry of an alloy influences its durability in the long-term hydriding-dehydriding cycles. A typical AB<sub>5</sub>-type alloy, available on the market and used in batteries, consists of at least six different metals, e.g. La<sub>0.64</sub>Ce<sub>0.36</sub>Nd<sub>0.46</sub>Ni<sub>0.95</sub>Cr<sub>0.19</sub>Mn<sub>0.41</sub>Co<sub>0.15</sub> (Hydralloy F) prepared at the Nürnberg plant (Germany) [31]. Important work in the field of hydrogen storage negative electrodes based on LaNi<sub>5</sub> has been done in Japan and the results are summarized by Sakai et al. [5].

#### AB-, A<sub>2</sub>B-, AB/AB<sub>2</sub>- and AB<sub>2</sub>-type alloys

In AB-, A<sub>2</sub>B-, AB/AB<sub>2</sub>- and AB<sub>2</sub>-type alloys, the component A represents elements belonging to Groups 3 or 4 of the Periodic Table, which form very stable hydrides, while the component B may be the transition metals from Groups 5-10, which determine the catalytic activity and chemical stability of an alloy (some of them do not form hydrides) [65, 66]. These alloys can roughly be arranged into two classes:

1. Type A<sub>2</sub>B, AB and AB/A<sub>2</sub>B based on Ti<sub>2</sub>Ni and TiNi [19, 23, 24, 67]; Beccu [23, 24] found a bell-shaped curve for hydrogen uptake with a maximum in the region where both alloys, TiNi and Ti<sub>2</sub>Ni, co-exist.
2. Type AB<sub>2</sub> (Laves-phase system) based on ZrNi<sub>2</sub>, ZrV<sub>2</sub> and ZrMn<sub>2</sub>; the AB<sub>2</sub> alloys crystallize in a cubic C15 and hexagonal C14 or C36 Laves phase structure [68] (Table 3).

So far the AB and A<sub>2</sub>B alloys have obtained only moderate importance as a consequence of a rather low specific capacity due to decomposition upon hydriding-dehydriding cycles. Better features, in particular for practical use as rechargeable battery electrodes, have been identified for AB<sub>2</sub>-type (Laves phase) alloys based on Zr-Ti-V-Ni. The latter multi-component alloys incorporate a lower amount of hydrogen per one molecule unit than the LaNi<sub>5</sub>-based alloys; however, owing to their attractive catalytic activity, the available rate capability of hydrogen sorption-desorption is considerably higher compared with that of other systems.

There have been many successful attempts to improve the behavior of the parent AB<sub>2</sub>-type intermetallic compounds as hydrogen storage materials by substituting part of the main elements, A and B. Significant improvements of the AB<sub>2</sub>-type alloys have been achieved by additives contributing to the

**Table 2** Effect of composition on properties of AB<sub>5</sub>-type alloys

Composition	Elements and their role	Ref
Substitutions of A in AB <sub>5</sub> : La <sub>1-y</sub> M <sub>y</sub> B <sub>5</sub>	Zr, Ce, Pr, Nd decrease the unit cell volume, improve activation, high-rate discharge and cycle life, but increase the self-discharge owing to a higher dissociation pressure of the metal hydride. The use of Mm instead of La reduces the alloy costs	[1, 5, 32, 33, 34, 35]
Substitutions of B in AB <sub>5</sub> : A(Ni <sub>1-z</sub> M <sub>z</sub> ) <sub>5</sub>	A = La, Mm; M = Co, Cu, Fe, Mn, Al; 0 < z < 0.24. Ni with (1-z) > 2.2 is indispensable to prevent the decrease of the amount of absorbed hydrogen and the electrode capacity. Co decreases the volume expansion upon hydriding, retards an increase of the internal cell pressure, decreases the corrosion rate and improves the cycle life of the electrode, especially at elevated temperature (40 °C), but increases the alloy costs. Substitution of Co by Fe allows cost reduction without affecting cell performance, decreases decrepitation of alloy during hydriding. Al increases hydride formation energy, prolongs cyclic life. Mn decreases equilibrium pressure without decreasing the amount of stored hydrogen. V increases the lattice volume and enhances the hydrogen diffusion. Cu increases high rate discharge performance	[36, 37, 38, 39, 40, 41]
Special additions to B in AB <sub>5</sub> : A(Ni,M) <sub>5-x</sub> B <sub>x</sub>	A = La, Mm; M = Co, Cu, Fe, Mn, Al; B = Al, Si, Sn, Ge, In, Tl. The metals Al, Si, Sn and Ge minimize corrosion of the hydride electrode. Ge-substituted alloys exhibit facilitated kinetics of hydrogen absorption/desorption in comparison with Sn-containing alloys. In, Tl, Ga increase overvoltage of hydrogen evolution (prevent generation of gaseous hydrogen)	[1, 42, 43, 44]
Non-stoichiometric alloys: AB <sub>5±x</sub>	A = La, Mm; B = (Ni,Mn,Al,Co,V,Cu). Additional Ni forms separate finely dispersed phase. In MmB <sub>5.12</sub> the Ni <sub>3</sub> Al-type second phase with high electrocatalytic activity is formed. Alloys poor in Mm are destabilized and the attractive interaction between the dissolved hydrogen atoms increases. Second phase (Ce <sub>2</sub> Ni <sub>7</sub> ), which forms very stable hydride, is present in MmB <sub>4.88</sub> . When (5-x) < 4.8 the hydrogen gas evolution during overcharge decreases	[30, 45, 46, 47, 48, 49, 50, 51, 52, 53, 54, 55, 56, 57, 58, 59, 60, 61, 62]
Addition of alloys with increased catalytic activity: AB <sub>5</sub> + DE <sub>3</sub>	D = Mo, W, Ir; E = Ni, Co. DE <sub>3</sub> is a catalyst for hydrogen sorption-desorption reactions	[63]
Mixture of two alloys: A <sup>1</sup> B <sup>1</sup> <sub>5</sub> + A <sup>2</sup> B <sup>2</sup> <sub>5</sub>	Mixing of two alloys characterized by various hydrogen equilibrium absorption pressures increases the electrode performance	[64]

**Table 3** Hydride forming alloys with Laves phase structures

	Examples	Lattice parameters		$r_A/r_B$
		$c$ (Å)	$a$ (Å)	
Hexagonal C14; HP12; $P6_3/mmc$ ; prototype: $MgZn_2$	ZrMn <sub>2</sub> , ZrCr <sub>2</sub> , TiMn <sub>2</sub>	7.9–8.3	4.8–5.2	1.225 (ideal); 1.12–1.26; coexistence with C36
Cubic C15; CF24; $Fd\bar{3}m$ ; prototype: Cu <sub>2</sub> Mg	TiCr <sub>2</sub> , ZrCo <sub>2</sub> , ZrMo <sub>2</sub> , ZrNi <sub>2</sub>	–	6.92–7.70	1.1–1.35
Hexagonal C36; HP24; $P6_3/mmc$ ; prototype: MgNi <sub>2</sub>	MgNi <sub>2</sub> , HfCr <sub>2</sub>	–	–	1.12–1.26; coexistence with C14

changes both in the unit cell volume and in the electronic structure, and, as a consequence, strongly affecting the stability and stoichiometry of the related hydrides [69]. A serious problem in the Zr-containing alloy system is the formation of a compact ZrO<sub>2</sub> layer on the sample surface. Owing to the low electrical conductivity of this oxide the transport of hydrogen into the catalytic sub-surface layer is impeded. This disadvantage can be eliminated by a partial replacement of Zr by Ti and/or Mn by Cr, but the hydrogen storage capacity of an alloy decreases with increasing additive content.

Typical AB<sub>2</sub>-type alloys for metal hydride electrodes are often not only multi-element but also multi-component and multi-phase systems. In a series of patents applied for between 1984 and 1995, all assigned to Energy Conversion Devices (Ovonic Battery Company) [70, 71, 72, 73, 74, 75, 76, 77, 78, 79, 80, 81, 82, 83, 84, 85], a multi-component AB<sub>2</sub>-type alloy, Zr<sub>0.55</sub>Ti<sub>0.45</sub>V<sub>0.55</sub>Ni<sub>0.88</sub>Cr<sub>0.15</sub>Mn<sub>0.24</sub>Co<sub>0.18</sub>Fe<sub>0.03</sub>, called the Ovonic alloy, is described. This is a multi-phase structure, which involves a specific grain phase for the reversible storage of hydrogen and a primary inter-granular phase capable of catalyzing oxidation of hydrogen. Many important manufacturers of Ni-MH batteries operate at present under agreements with the Ovonic Battery Company. Ovonic Ni-MH electric vehicle battery packs have been installed on a number of prototype electric vehicles, like Solectria and Chrysler's Tevan. Nevertheless, there is a problem with the activation of the Ovonic alloy during the first cycles of operation [4, 86, 87, 88] and recent studies regarding similar alloy compositions have focused on solving this problem [89, 90, 91, 92]. The hydriding-dehydriding behavior of AB<sub>2</sub>-type alloys is strongly influenced by their composition and stoichiometry, as well as by the microstructure of the material particles and the presence of additives and impurities [69, 70, 71, 72, 73, 74, 75, 76, 77, 78, 79, 80, 81, 82, 83, 84, 85, 86, 87, 88, 89, 90, 91, 92, 93, 94, 95, 96, 97, 98, 99, 100, 101, 102, 103, 104, 105, 106, 107, 108, 109, 110, 111, 112, 113, 114, 115, 116, 117, 118, 119, 120] (see also Table 4). An excellent explanation of the role of various different additives in modification of the properties of hydride-forming alloys has been given by Doi and Yabuki [116, 117].

### Selection of alloys for battery applications

For application purposes in batteries and battery-related fields, hydrogen storage alloys must be characterized by a high hydrogen capacity and moderate hydride stability, as well as by an almost constant equilibrium pressure during the solid phase (MH<sub>α</sub> to MH<sub>β</sub>) conversion and a low sorption-desorption hysteresis. Usually, information about these properties is inferred from pressure vs. concentration (PC) isotherms (sometimes called PCT characteristics), providing the dependence of the equilibrium pressure of hydrogen,  $p(H_2)$ , on the amount of hydrogen dissolved and/or incorporated in the solid phase at various constant temperatures. Furthermore, the PC isotherms are used to reveal various hydride phases of alloy compounds. There are also some common criteria for the selection of constituents in a hydride alloy composition, which are based on the physical properties of individual elements and their hydrides (electronic structure, atomic bond radius and unit cell volume) ([69] and references therein).

The heat of hydride formation ( $\Delta H$ ) is an important parameter characterizing the alloy as a proper hydrogen absorber for various specific applications. Ovshinsky et al. [122] have stated that if the  $\Delta H$  value ranges between –25 kJ/mol and –50 kJ/mol, the alloy is suitable for battery applications. Hong [121] has postulated that the heat of alloy hydride formation should be between –15 kJ/mol and –40 kJ/mol. When it is lower than –15 kJ/mol, then the alloy hydride is not stable enough for charging the MH electrode at room temperature. On the other hand, the alloy hydride is too stable for the room-temperature discharge when the  $\Delta H$  value exceeds –40 kJ/mol.

The nature of components and their ratio in the designed hydrogen absorbing alloy, A<sub>a</sub>B<sub>b</sub>C<sub>c</sub>, can be assessed as follows [121]:

$$\Delta H = [a\Delta H_{AH} + b\Delta H_{BH} + c\Delta H_{CH} + \dots]/(a + b + c + \dots) \quad (2)$$

where  $\Delta H_{AH}$ ,  $\Delta H_{BH}$ ,  $\Delta H_{CH}$  are heats of formation of individual metal hydrides (see Table 5).

The enthalpy ( $\Delta H$ ) and, furthermore, the entropy ( $\Delta S$ ) of hydride formation can be derived from the

**Table 4** Effect of composition on properties of AB- and AB<sub>2</sub>-type alloys

Composition	Elements and their role	Ref
ZrM <sub>2</sub> -type alloy. M = V, Cr, Mn, Ni. Zr(V <sub>x</sub> Ni <sub>1-x</sub> ) <sub>2</sub>	An increase of the V content increases the maximum amount of absorbed hydrogen. Ni substitution decreases the electrochemical activity of an alloy	[97]
ZrB <sub>2</sub> -type alloy. ZrNi <sub>1.2</sub> Mn <sub>0.6</sub> V <sub>0.2</sub> Cr <sub>0.1</sub> X <sub>x</sub> . Over-stoichiometric alloy: ZrV <sub>1.5</sub> Ni <sub>1.5</sub>	Composite alloy, mixture of ZrNi <sub>2</sub> with RNi <sub>5</sub> (R = rare earth element), shows improved characteristics in comparison with the parent compounds X = La or Ce; x = 0.05. La and Ce do not dissolve in the Laves phase but precipitate in the matrix, improve the activation behavior of alloy during chemical pretreatment and increase discharge capacity In stoichiometric AB <sub>2</sub> -type alloy the distribution of A and B elements on the A and B sites is crucial for high hydrogen storage capacity; the over-stoichiometric alloy, in which some of the V atoms move from B to A sites, shows very high capacity	[108] [105] [110]
TiFe-type alloy: TiFe <sub>1-x</sub> Pd <sub>x</sub>	Pd substitution increases both the lattice constant and the catalytic activity, decreases the plateau pressure	[106]
Vanadium-based alloys: V <sub>3</sub> Ti(Ni <sub>1-x</sub> M <sub>x</sub> ), V <sub>3</sub> TiNi <sub>x</sub> M <sub>y</sub>	M = Al, Si, Mn, Fe, Co, Cu, Ge, Zr, Nb, Mo, Pd, Hf, Ta. Phase structure is composed of the V-based solid solution as the main phase and the TiNi-based secondary phase; the addition of Co, Nb and Ta improves cycling durability	[104]
Substitution of A in AB <sub>2</sub> ; A = Zr + Ti: Ti <sub>x</sub> Zr <sub>1-x</sub> Ni <sub>1.1</sub> V <sub>0.5</sub> Mn <sub>0.2</sub> Fe <sub>0.2</sub>	Alloys with Hf (or Nb), Ta and Pd show higher discharge capacity. M = Hf improves the high rate capability. TiNi phase exhibits high electrocatalytic activity Zr contributes to an increase of the amount of stored hydrogen and induces formation of the C15-type desired phase structure. Ti increases the equilibrium pressure of hydrogen and decreases the electrochemical capacity	[109] [93]
Substitution of B in AB <sub>2</sub> ; Zr <sub>0.8</sub> Ti <sub>0.2</sub> (V <sub>0.3</sub> Ni <sub>0.6</sub> M <sub>0.1</sub> ) <sub>2</sub> , Ti <sub>0.35</sub> Zr <sub>0.65</sub> Ni <sub>1.2</sub> V <sub>0.6</sub> Mn <sub>0.2</sub> Cr <sub>0.2</sub>	Electrodes without Ti, or a very low Ti content, exhibit excellent cycling and electrochemical stability Electrodes with Ti:Zr atomic ratio 2:1 display higher storage capacity than that with Ti:Zr = 1:1, and higher electrochemical activity Amount of C15 phase decreases with increasing x; at x = 0.5 it is pure C14 phase, at x = 0.75 it is 13% cubic bcc phase + 87% C14 phase; bcc phase absorbs more hydrogen than the C14 hexagonal phase The Si, Mn-substituted alloys has C14 Laves phase structure. The Co, Mo-substituted alloys form C15 Laves phase structure Mn enhances the activation of an alloy during chemical pretreatment and increases discharge capacity. Co addition leads to the longest cyclic lifetime. Cr addition reduces the discharge capacity but extends cyclic lifetime; Cr controls the dissolution of V and Zr	[103, 107] [111] [102] [112] [113]
Non-stoichiometric alloys AB <sub>2±x</sub> : Zr <sub>0.495</sub> Ti <sub>0.505</sub> V <sub>0.771</sub> Ni <sub>1.546</sub> , Ti <sub>0.8</sub> Zr <sub>0.2</sub> Ni <sub>0.6</sub> V <sub>0.64</sub> Mn <sub>0.4</sub> , ZrV <sub>0.8</sub> Ni <sub>1.2</sub> Mn <sub>0.4</sub>	Increasing the Ni content decreases V-rich dendrite formations C14-type Laves phase preserves an over-stoichiometric alloy and discharge capacity increases on increasing the amount of Ni	[89] [98]
MgNi-based alloys for electrodes. Optimum ternary alloy: Mg <sub>50</sub> Ni <sub>45</sub> M <sub>5</sub> (M = Mn, Cu, Fe)	Ni substitution with Zn increases the deterioration rate. Substitution of Fe, W, Cu, Mn, Cr, Al or C instead of Ni decreases both the deterioration rate and discharge capacity. Ni substitution by Se, Cu, Co or Si decreases both the discharge capacity and cycling life	[114]

temperature dependence of the hydrogen adsorption-desorption isotherms by using the van't Hoff relation:

$$\ln[p(\text{H}_2)/p^\circ] = \Delta H/RT - \Delta S/R \quad (3)$$

where  $p(\text{H}_2)$  is the equilibrium hydrogen pressure upon  $\alpha$  to  $\beta$  hydride phase conversion;  $p^\circ$  is the standard pressure,  $R$  is the gas constant and  $T$  is the temperature.

It was found that the C14-type Laves phase structure with a large unit cell volume is formed in the multi-component Zr- and Ti-based alloys if the electron densities in the dsp and d orbitals are about 7 and 4.4, respectively (Table 6) [79, 89, 115]. The basic C14 phases, TiMn<sub>2</sub> and TiCrMn, are themselves not suitable for the intended applications in Ni-MH batteries because the unit cell volume of their crystal lattice is so small in both cases that a hydride phase can be formed only at very low temperatures. An important step in the

improvement of hydride stability and hydrogen capacity in the investigated system is the expansion of the crystal lattice by incorporating Zr, which has a larger metallic radius than the parent elements [115].

The best way to attain fast kinetics for the hydrogen electrode reactions is to enhance the intrinsic properties of the alloy. Therefore, it is important to define the activities of each of the alloying elements regarding the hydrogen evolution and/or oxidation reaction. To improve the catalytic activity of hydrogen storage materials in alkaline solution, specially selected metal alloys (so-called "Brewer" alloys) were predicted as additives by taking into account the Brewer-Engel theory of the electronic structure of intermetallic compounds in the main alloy phase. These small additives should be characterized by a higher melting point than the main phase and by an ability to form intermetallic compounds

**Table 5** Characteristics of individual elements used in AB/AB<sub>2</sub> alloys for metal hydride electrodes

No. in Periodic Table	Element	Mass number	Atomic radius (Å)	Density (g/cm <sup>3</sup> )	Melting point (°C)	Valence electrons	Heat of hydride formation (kJ/mol)	log <i>j</i> <sub>0</sub> (A/cm <sup>2</sup> )	Valence
13	Al	27	1.41	2.38	660	3s <sup>2</sup> 3p <sup>1</sup>	-7 (AlH <sub>0.5</sub> ), -4 (AlH <sub>3</sub> )	10	3
22	Ti	48	1.488	4.50	1677	3d <sup>2</sup> 4s <sup>2</sup>	-68 (TiH <sub>2</sub> )	8.3	4, 3
23	V	51	1.355	5.87	1917	3d <sup>3</sup> 4s <sup>2</sup>	-35 (VH <sub>0.5</sub> )	-	5, 4, 2
24	Cr	52	1.285	7.14	1903	3d <sup>5</sup> 4s <sup>1</sup>	-6 (CrH), -8 (CrH <sub>0.5</sub> )	11	6, 3, 2
25	Mn	55	1.366	7.30	1244	3d <sup>5</sup> 4s <sup>2</sup>	-8 (MnH <sub>0.5</sub> )	8.6	7, 4, 2, 6, 3
26	Fe	56	1.26	6.90	1535	3d <sup>6</sup> 4s <sup>2</sup>	+10 (FeH <sub>0.5</sub> )	5.5	3, 2
27	Co	59	1.25	8.71	1495	3d <sup>7</sup> 4s <sup>2</sup>	+15 (CoH <sub>0.5</sub> )	5.2	3, 2
28	Ni	58	1.246	8.90	1455	3d <sup>8</sup> 4s <sup>2</sup>	-3 (NiH <sub>0.5</sub> )	5	2, 3
29	Cu	63	1.275	8.93	1083	3d <sup>10</sup> 4s <sup>1</sup>	+46 (solut.)	6.3	2, 1
40	Zr	90	1.60	6.40	1852	4d <sup>2</sup> 5s <sup>2</sup>	-82 (ZrH <sub>2</sub> )	-	4
41	Nb	93	1.47	8.57	2500	4d <sup>4</sup> 5s <sup>1</sup>	-38 (NbH <sub>0.5</sub> )	8.5	5, 3
42	Mo	98	1.40	9.01	2620	4d <sup>5</sup> 5s <sup>1</sup>	+5 (MoH <sub>0.5</sub> )	-	6, 3, 5
57	La	138.91	1.38	6.17	918	5d <sup>0</sup> 6s <sup>2</sup>	-97 (LaH <sub>2</sub> )	-	-3
72	Hf	180	1.585	11.4	1975	5d <sup>2</sup> 6s <sup>2</sup>	-66 (HfH <sub>2</sub> )	-	4

**Table 6** Discharge capacity of selected AB<sub>2</sub> alloys with C14 Laves phase structure [115]

Alloy	Number of electrons in dsp orbitals	Number of electrons in d orbitals	Discharge capacity (mAh/g)	Cell volume, Δ <i>V</i> (Å <sup>3</sup> )
Zr <sub>0.65</sub> Ti <sub>0.35</sub> Ni <sub>1.0</sub> V <sub>0.8</sub> Mn <sub>0.4</sub>	6.50	4.50	230	173.17
Zr <sub>0.65</sub> Ti <sub>0.35</sub> Ni <sub>1.2</sub> V <sub>0.6</sub> Mn <sub>0.2</sub>	6.80	4.80	247	171.91
Zr <sub>0.65</sub> Ti <sub>0.35</sub> Ni <sub>1.2</sub> V <sub>0.4</sub> Mn <sub>0.4</sub>	6.93	4.93	210	170.76
Zr <sub>0.65</sub> Ti <sub>0.35</sub> Ni <sub>0.6</sub> V <sub>1.4</sub>	6.60	3.66	-	Three-phase alloy

with Ni and Co. Fundamental work in this field has been published by Jaksic [63]. Some examples of Brewer metal alloys are given in Table 7.

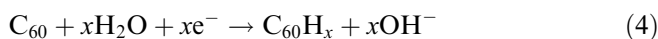
Detailed information about the properties of individual elements used in the preparation of Ti-Zr-V-Ni- and LaNi<sub>5</sub>-based hydride alloys are helpful in choosing the appropriate component composition (Table 8).

### Fullerenes and their hydrides

Fullerenes are synthesized in the gas phase at relatively high temperatures, where carbon atom clusters are formed with compositions from C<sub>2</sub> to C<sub>18</sub>. These tend to further assemble into fullerene molecules: C<sub>60</sub>, C<sub>70</sub>, C<sub>84</sub>, etc. [17]. The fullerene structure was first predicted

theoretically by Osawa in 1970 [123], but it was not experimentally found until much later, in 1985, by Kroto et al. [124]. The synthesis and separation of fullerenes was done by Krätschmer et al. in 1990 [17].

A spherical cyclic alkene chain of fullerene, C<sub>60</sub>, contains 30 conjugated double bonds with a variety of closed and open graphene architectures. So far, fullerenes have found various applications in optics, chemical catalysis, sensors, batteries, fuel cells, gas storage, separation science and as a host for other molecules. The electrochemical hydrogenation of fullerenes can be written as follows:



For the completely hydrogenated fullerene, C<sub>60</sub>H<sub>60</sub>, the theoretical capacity is 2234 mAh/g with a volumetric capacity of 3820 mAh/cm<sup>3</sup>. Theoretical calculations show that the most stable hydrogenated products of C<sub>60</sub> are C<sub>60</sub>H<sub>24</sub>, C<sub>60</sub>H<sub>36</sub> and C<sub>60</sub>H<sub>48</sub>. Owing to its unique molecular structure, fullerene is the only form of carbon which potentially can be chemically hydrogenated and de-hydrogenated reversibly [17]. The 30 double C=C bonds on each C<sub>60</sub> sphere could be opened up to form C-H bonds under certain conditions; theoretical heats of formation for C<sub>60</sub> and C<sub>60</sub>H<sub>36</sub> are 890 and 330 kcal/mol, respectively. Thin film fullerene (C<sub>60</sub>/C<sub>70</sub>) electrodes on various substrates have been investigated [17], and a discharge capacity of about 1600 mAh/g, corresponding

**Table 7** "Brewer" alloys proposed for activation of metal hydride alloys [63]

Alloy	Structure	Temperature of formation (°C)
Ni <sub>3</sub> Mn	Fcc	620
NiMn	tetrag	900
Ni <sub>3</sub> Fe	Fcc	480
Ni <sub>3</sub> Cr	Fcc	800
Ni <sub>3</sub> V	Fcc	1050
Ni <sub>4</sub> Mo; Ni <sub>3</sub> Mo; Co <sub>3</sub> Mo	tetrag	-
Ni <sub>6</sub> W; Ni <sub>3</sub> W; Co <sub>3</sub> W	-	980

**Table 8** Properties of individual elements for AB<sub>5</sub> and AB<sub>2</sub> alloys [1, 5, 32, 33, 34, 35, 36, 37, 38, 39, 40, 41, 42, 43, 44, 45, 46, 47, 48, 49, 50, 51, 52, 53, 54, 55, 56, 57, 58, 59, 60, 61, 62, 63, 64, 69, 70, 71, 72, 73, 74, 75, 76, 77, 78, 79, 80, 81, 82, 83, 84, 85, 86, 87, 88, 89, 90, 91, 92, 93, 94, 95, 96, 97, 98, 99, 100, 101, 102, 103, 104, 105, 106, 107, 108, 109, 110, 111, 112, 113, 114, 115, 116, 117, 117, 120]

Element	Selected properties
La and Mm	Forms stable hydrides ( $\Delta H = -97$ kJ/mol for LaH <sub>2</sub> ) Improves the electrochemical behavior of AB <sub>5</sub> and AB <sub>2</sub> alloys
Zr	Forms stable hydrides ( $\Delta H = -82$ kJ/mol for ZrH <sub>2</sub> ) Absorber of gaseous O <sub>2</sub> , N <sub>2</sub> , CO <sub>2</sub> , etc. Oxidizes quickly, forming compact passive oxide layer; increasingly loose when alloyed with Ti
Ti	High electrocatalytic activity Forms stable hydrides ( $\Delta H = -68$ kJ/mol for TiH <sub>2</sub> ) Complete solubility with Zr Inhibits Zr oxidation Oxidizes, forming loose passive oxide layer Dissolution in KOH When Ti replaces for Zr in AB <sub>2</sub> alloy, the plateau pressure of hydrogen increases, hydrogen absorption capacity becomes smaller, but hysteresis in the PC isotherms decreases
V	Forms stable hydrides ( $\Delta H = -35$ kJ/mol for VH <sub>0.5</sub> ) On B site in AB <sub>2</sub> structure, improves hydrogen sorption capacity and kinetics When on A site in AB <sub>2</sub> , the alloy hardly absorbs hydrogen Both in AB <sub>5</sub> and AB <sub>2</sub> alloys forms oxides soluble in alkaline solution Increases the alloy surface owing to dissolution in alkaline solution
Ni	Forms unstable hydride ( $\Delta H = -3$ kJ/mol for NiH <sub>0.5</sub> ) Indispensable element because of its high electrocatalytic activity Forms intermetallics, decreases the Me-H bond strength to a suitable level Sensitive to corrosion and oxidation during cycling [forms Ni(OH) <sub>2</sub> ] Decreases oxidation of Zr-Ti-V alloys and increases the discharge capacity Excessively high Ni content leads to decrease in the discharge capacity
Cr	Forms unstable hydride ( $\Delta H = -6$ kJ/mol for CrH, $\Delta H = -8$ kJ/mol for CrH <sub>0.5</sub> ) Inhibitor of vanadium corrosion Influences on M-H bond strength in alloy Good cycling properties Easily forms TiCr <sub>2</sub> and separate bcc phase with vanadium Is not easily introduced in C14 phase
Fe	Does not form hydrides (positive enthalpy of hydride formation, $\Delta H = +10$ kJ/mol for FeH <sub>0.5</sub> ) Exhibits catalytic activity in hydrogen evolution from water solutions Soluble in concentrated alkaline solution: forms oxo anions In an electrolyte can be detrimental to the poisoning of nickel hydroxide Increases plateau pressure of hydrogen absorption
Mn	Forms unstable hydride ( $\Delta H = -8$ kJ/mol for MnH <sub>0.5</sub> ) Enhances the pulverization of an alloy Increases the mutual solubility of the other elements during solidification Substitution of Ni by Mn on the B site decreases the plateau equilibrium pressure of hydrogen, but hysteresis in the PC isotherm becomes larger Increases the electrode surface by dissolving in alkaline solution Catalyst (in the form of multivalent oxides, especially when Fe is absent)
Co	Addition of 6–8 at% to alloy results in increased hydrogen storage capacity, low cell pressure, high cycle life Does not form hydrides ( $-\Delta H = +15$ kJ/mol for CoH <sub>0.5</sub> ) Decreases the dissolution of Mn (in AB <sub>5</sub> ) Improves the cycle life, decreases hydrogen absorption rate Rises plateau pressure of hydrogen absorption in an alloy Exhibits catalytic activity (Co <sub>3</sub> Mo) in hydrogen evolution
Al	Forms unstable hydrides ( $\Delta H = -7$ kJ/mol for AlH <sub>0.5</sub> , $\Delta H = -4$ kJ/mol for AlH <sub>3</sub> ) Decreases the plateau pressure (in AB <sub>5</sub> )
Mo, B, Ta, W, Zr	Improve the electrochemical activity of the alloys AB <sub>5</sub> and AB <sub>2</sub>

to C<sub>60</sub>H<sub>48</sub>, was measured. This is about four times higher than for any metal hydride. Another advantage of using the fullerene hydride system might be a very fast charging time. Unfortunately, the cycle life of actual fullerene electrodes is rather poor.

#### Alloy preparation

Hydride forming alloys (especially the AB<sub>2</sub>-type) are characterized by high melting points and therefore two

types of furnaces, namely arc melting and induction, are used for their melting. In a small-scale production, where it is necessary to melt a great number of various alloy compositions, e.g. in laboratories, direct arc melting is used. In this method, a pressed pellet (from powders of different metals mixed together) is melted by direct contact with an electric arc in argon atmosphere.

The arc melting technique provides two main advantages over other melt processes: (1) great versatility in terms of the types of materials, and (2) limited reactivity during melting. The disadvantages of the arc

melting method are as follows: (1) low efficiency and hazardous preparation conditions; (2) for multi-component alloys, multiple re-melting or prolonged annealing at high temperature is necessary in order to obtain a homogenous distribution of components throughout the volume of the pellet.

Electrically powered induction furnaces are used for large-scale alloy production. This method is convenient because bulk raw materials can be used instead of powders and step-by-step addition of components can be performed. The molten metal is poured from the furnace by tilting or tapping the furnace and the metal is then passed to the molds or different vaporizers.

A typical preparation scheme of the AB<sub>5</sub>-type alloys, as described by a number of authors [30, 34, 36, 53, 54], includes: (1) mixing the chosen materials in the given ratio and pressing into pellets; (2) melting in an inert atmosphere (argon) using arc or induction furnaces; (3) fast cooling; and (4) crushing mechanically or using hydrogen gas sorption-desorption cycles.

The production of the AB<sub>2</sub>-type alloys, according to reports by the Ovonic company [73, 74, 75, 76, 77, 78, 79, 80, 82, 86], involves the following steps: (1) mixing of starting components; (2) placing into a high-temperature furnace and evacuating it to a pressure of 10<sup>2</sup> N m<sup>-2</sup>; (3) purging with argon and heating to the temperature sufficient to melt the alloy; (4) mixing of additives with the melt (if necessary) and removing impurity slag and oxides; (5) prolonged annealing in a vacuum or an argon atmosphere at temperatures close to the melting point, where homogenization proceeds; (6) cooling of solid ingot form prior to removal from the autoclave; (7) comminution using hydrogenation in a vacuum pressure vessel followed by cooling in an inert atmosphere (Ar); and (8) further comminution with ball milling in an inert atmosphere and at low temperature.

### Amorphous metal alloys

Amorphous metal alloy materials have gained great interest since the 1980s owing to their unique combinations of mechanical, chemical and electrical properties. This might be attributed to the disordered atomic structure that ensures chemical homogeneity and the lack of extended defects in these materials. Hydrides made of the amorphous metal alloys are sometimes capable of absorbing larger amounts of hydrogen than their crystalline counterparts under similar experimental conditions (for example, TiCu and ZrCu). Sapru et al., Grasselli et al. and others [75, 125, 126, 127, 128, 129, 130, 131] used amorphous alloys to prepare hydrogen-absorbing electrodes. Different amorphous electrode materials have been tested for application in electrochemical power cells, including Ni-Mg alloys, which typically cannot be charged electrochemically. Disordered metal alloys, useful for the preparation of the hydrogen-absorbing electrodes, can be obtained in different ways using electron beam deposition, ion

implantation, chemical reduction, thermal decomposition, ion cluster deposition, ion plating, liquid quenching, gas atomization, solid state diffusion, RF and DC sputtering and mechanical alloying [124, 125, 126, 127, 128, 129, 130, 131, 132, 133, 134, 135, 136, 137].

The discoveries of the technical possibilities and methods mentioned above allowed production of hydrogen-absorbing electrodes from the lightest metals, like Mg and Li, which are known to form hydrides with the highest available capacity. Until that time, they were not actively developed owing to chemical and metallurgical problems, electrochemical instability, etc. Mg-Ni based materials appeared to be more amenable to rapid solidification and mechanical alloying techniques. The latter technique opened up new possibilities for the syntheses of materials from elements previously not compatible, i.e. Mg-La-Ni [136, 137]. Some of these techniques will be discussed below.

### *Pulverizing from the melt (gas atomizing method)*

The hydrogen-absorbing alloy particles of uniform size were manufactured from the melt by a pulverizing method [126, 127, 128, 129, 130, 131, 132]. A molten alloy was supplied in vacuum (or under cooling gas atmosphere) to the running surface of a rotor moving at a high speed. This dispersed the molten hydrogen-absorbing alloy in the form of very fine particles (by the kinetic energy of the rotor) and, at the same time, solidified it rapidly. The surfaces of such grains are smooth, without edges or ridges. The methods used for fast cooling include rotary disk, rotary nozzle, single and twin roll, and the inert gas atomizing method. The gas atomizing method was analyzed theoretically by Grasselli et al. [127] in application to the formation of amorphous metal alloys A<sub>a</sub>B<sub>b</sub>M<sub>c</sub>N<sub>d</sub> (A=Pt, Pd; B=Zr, Ti, Ca, Mg; M=Ni, Co, Mn; N=Zr, Ti, Ca, Mg, N, C, Ge, P, As, Sb, Pb, Sn, Si, W). The incorporation of component A in the composition protected the surface from passivation and made the product more active in the hydrogen absorption-desorption reaction. The incorporation of the fourth component, N, in this composition ensured easier formation of the amorphous phase. Based on the hydriding characteristics of some AB<sub>5</sub> alloys produced by high-pressure gas atomization [129], it was found that hydrogen gas storage capacities and the equilibrium pressures are nearly identical to the alloys prepared from an ingot. Alternatively, Lim et al. [128] reported that atomized alloys show lower specific capacity and slower activation with cycling than the corresponding non-atomized alloys.

### *Thin amorphous films*

Sputter deposition of AB<sub>5</sub>-based alloys to obtain amorphous films was used by Sakai et al. [134] and Li



and Cheng [135]. The presence of Mn in the alloy influenced the formation of microcrystalline films. Sapru et al. [125] and Machida et al. [197] investigated Ti-Ni thin film electrodes and observed very high electrocatalytic activity due to a well-developed active surface and the electrocatalytic activity of Ni. Recently, Mg-Ni based thin films (1–3  $\mu\text{m}$ ) were deposited on Ni substrates using a RF sputtering method [136]. The compositions  $\text{Mg}_{54}\text{Ni}_{42}\text{Co}_4$  and  $\text{Mg}_{52.3}\text{Ni}_{45.2}\text{Co}_{2.5}$  showed the highest available capacities, 408 mAh/g and 629 mAh/g, respectively. However, the degradation during cycling was very rapid.

#### *Mechanical alloying method*

This method of producing hydrogen-absorbing alloys was introduced a few years ago [129, 137, 138, 139, 140, 141, 142, 143, 144, 145, 146, 147]. The formation of a metal hydride during the ball milling process was first observed by Chen and Williams ([138] and references therein). They found the formation of a  $\text{TiH}_{1.9}$  phase in the early stage of Ti milling in ammonia. This suggested that mechanical alloying could probably be a simple method for the production of metal hydride powders with any composition. The starting materials for ball milling are elemental powders, and the reaction atmosphere used is hydrogen or argon. Especially hardened steel balls were used and typical milling times were from 10 to 100 h. The observed decrease in hydrogen pressure during the first hours of milling of the pure metals (Zr, Ti, Mg, etc.) and/or their composites showed substantial absorption of hydrogen into the metal particles. Typical dimensions of the alloy particles after prolonged milling (at least 20 h) were under 1  $\mu\text{m}$ . Because as-cast Zr-Ti-Ni based alloys showed slow activation, the composite particles with pure nickel on the surface of a Zr-Ti based Laves phase compound were prepared by means of mechanical ball milling [140, 143, 144]. X-ray analysis revealed that nickel particles were situated on the surface of the  $\text{AB}_2$  alloy grains and, at the same time, some fresh surfaces were simultaneously generated. This not only increased the discharge capacity but also the activation in alkaline electrolyte. Ti-Fe alloys showed an amorphous state after 40 h of ball milling, whereas Zr-Cr alloys revealed a mixture of nanocrystalline  $\text{ZrCr}_2$  and an amorphous state [143]. Alloys of magnesium have high gravimetric capacities but at the present time there are no known methods for the application of these electrodes in rechargeable batteries. Recently, use of the mechanical alloying method showed that it is possible to make alloys of most materials, including Mg [130, 141, 145]. Electrochemical measurements indicated that only an amorphous phase in  $\text{Mg}_x\text{Ni}_{100-x}$  alloys could electrochemically absorb and desorb hydrogen at room temperature [145], with capacities over 350 mAh/g.

#### Sintered, non-sintered and Raney-type M/MH electrodes

The practical energy densities of electrode materials used in energy storage device electrodes are always lower compared to the theoretical values because finite amounts of binders and conductive particles are necessary to enhance the electrical and mechanical properties. Generally, to characterize the overall electrochemical properties of the metal hydride electrode, all constituents should be taken into account. For example, it is known that nickel and copper, two typical additives for metal hydride electrodes, also form hydrides themselves [148, 149, 150].

Non-sintered electrodes are mostly formed using  $\text{AB}_5$ -type alloys [7, 18, 32, 34, 43, 44, 49, 50, 51, 151, 152]. To prepare negative electrodes with a satisfactory performance, the hydrogen-absorbing alloy particles (grains with dimensions 20–30  $\mu\text{m}$ ) are mixed with binder (ranging from 0.1 to 7 wt%) and an electrically conductive material (from 0.1 to 4 wt%) and a slurry is then formed, fixed to the current collector. Polyacrylates (sodium, ammonium or potassium polyacrylate), fluorine resins [polytetrafluoroethylene (PTFE)], aqueous poly(vinyl acetate) (PVA) solution and carboxymethyl cellulose (CMC) are the most used binder materials. The electrically conductive materials usually used are activated carbon, acetylene black, graphite and nickel and/or copper powders. The electrically conductive admixture present in an anode can be formed on a two-dimensional structure such as a punched metal or expanded metal mesh, or on a three-dimensional structure like a foamed metal, sponge nickel (porosity 90%), mesh-like metal fiber or flake-type copper or nickel powder, thus forming a laminated network structure during pressing [52, 152].

The electrochemical performance of metal hydride electrodes is strongly influenced by the initial particle size of the alloy powder, by the type and the amount of the conductive additive and also by the thickness of the electrode [153, 154, 155, 156]. For example, an  $\text{AB}_2$  electrode with 1 wt% carbon black has better stability than the same electrode with 20 wt% Ni powder [154]. Züttel et al. [153] compared two powders (Cu and Ni) as conductive materials for metal hydride electrodes. The heat conductivity of nickel is about five times smaller than that of copper, whereas the electrical resistivity is higher and nickel is more sensitive to oxidation than copper.  $\text{AB}$ - and  $\text{AB}_2$ -type Laves phase alloys are mainly subjected to the sintering process [56, 75, 77, 81]. In this process an alloy powder is mixed with a sintering component (2–10 wt% of nickel powder or nickel carbonyl) and a binder resin [i.e. polyethylene, CMC, poly(vinyl alcohol) (PVA)] added until a homogeneous paste is obtained. Then, the paste is placed in a conductive core material and dried in vacuum, pressed, molded and finally sintered in vacuum at a temperature of 700–1200  $^\circ\text{C}$ . During sintering, the resin binder is thermally decomposed at 400  $^\circ\text{C}$ .

In 1965, Wolf [21] patented an alkaline battery with a Raney-metal hydrogen electrode. He founded that freshly activated Raney nickel could contain hydrogen in atomic form which corresponds to the compound  $\text{Ni}_2\text{H}$ , rather than to  $\text{NiH}$ . The "Raney metal structure" represents a three-dimensional porous structure which is formed by two components dissolving one in the other. Possible active metal components of a Raney electrode are Fe, Co, Ni or Pd, whereas inactive components are Al, Zn or Mg. For example, Beccu and Siegert [19] prepared a Raney-type electrode from  $\text{TiNi}$  and  $\text{TiNi}_3$  alloys.  $\text{TiH}_2$  powder (particles with diameter less than  $20\ \mu\text{m}$ ), Ni powder ( $d < 40\ \mu\text{m}$ ) and sodium silicate as starting components were mixed to form the paste and coated on a Ni substrate. After drying and annealing in a  $\text{H}_2$  atmosphere at  $900\ ^\circ\text{C}$ , the sodium silicate was dissolved with a  $\text{NaOH}$  solution (10%). Wojcik et al. [160, 161] optimized the composition of a Ni-Al alloy to make a Raney-type hydrogen storage electrode. It should be noted that the volume of hydrogen electro-sorbed in the nickel electrode depends greatly on the preparation method and the presence of surface poisons. These effects were studied by Baranowski and Smialowski [157, 158, 159].

A composite-coated metal hydride electrode was proposed by Kleperis et al. [161, 162], based on the well-known composite-coated electrodes used for water electrolysis [163, 164, 165]. During plating, the hydrogen-absorbing alloy particles were co-deposited on the cathode together with the electroplated nickel and a uniform layer was obtained. As a result of this procedure the following goals were achieved: (1) the effective encapsulation of the alloy particles and (2) the presence of a catalytically active material on the surface of the alloy particles (electroplated nickel [148]). Preliminary results showed that only the electrodes with the  $\text{AB}_5$ -type alloy could be charged with hydrogen in this composite layer.

Studies on the charge-discharge efficiency of metal hydride electrodes based on La and Mm (i.e. [1, 3, 7]) showed that oxide formation, dissolution of selected elements (by decomposition or chemical disproportionation) and the pulverization of an alloy are the three most serious problems in using the hydride electrodes. A simple solution to these problems was to enrich the grain surface with catalytically active compounds (platinum black,  $\text{Ni}_3\text{M}$  ( $\text{M} = \text{W}, \text{Mo}, \text{Mn}, \text{V}$ ) [7, 63]) or to perform microencapsulation (see, e.g. [7]). The encapsulation method was introduced to preserve the alloy grains from disintegration due to volume changes occurring during the charge-discharge cycling, and to keep the surface electrochemically active. Electroless coating methods for nickel, copper and duplex nickel ( $\text{Ni-P} + \text{Ni}$ ) were applied to preserve  $\text{AB}_5$  as well as  $\text{AB}_2$  alloys [7, 166, 167, 168]. The main deficiency of  $\text{AB}_2$  alloys (including Ovonic alloys) is their difficult activation in the first cycles. Although the Ni and Cu coatings for the  $\text{AB}_2$  alloys were shown by Jung et al. [169] to be very useful, despite the activation problems, most other researchers use

activation of  $\text{AB}_2$  alloy particles in hot alkali [3, 4, 91, 101, 169, 170].

The surface treatment of metal hydride electrodes plays an important role in the performance characteristics (discharge capacity, cyclic life stability). A slow pretreatment activation rate of Zr-based  $\text{AB}_2$  metal hydride electrodes is one of the reasons for their slow commercialization. Also the performance of  $\text{AB}_5$ -type metal hydride electrodes needs further improvement. Therefore, a number of papers have been devoted to the activation and surface properties of metal hydride electrodes [166, 167, 168, 169, 170, 171, 172, 173, 174, 175, 176, 177, 178, 179, 180, 181, 182, 183, 184, 185, 186, 187, 188]. Recently, fluorination of hydrogen storage alloys was found to be effective for the improvement of the durability and the initial discharge characteristics of hydride electrodes [17, 178]. Fluoride layers on an alloy surface contribute to the selective permeability of hydrogen molecules in the gas-solid reaction and provide a protective barrier against impurities such as water vapor, carbon oxides, air and others. For the  $\text{AB}_2$ - and  $\text{AB}_5$ -type alloy electrodes, the fluorination process considerably improves the initial charge-discharge characteristics (removal of the oxide layer from the surface) as well as the durability of the MH electrodes. A new technique was developed by Sakashita et al. [178] to implant metallic Ni in the fluoride layer. Some methods have been proposed for improving the pretreatment of alloys [1, 2, 3, 4, 5, 6, 7, 8, 9, 10, 11, 12, 13, 14, 15, 16, 17, 18, 19, 20, 21, 22, 23, 24, 25, 26, 27, 28, 29, 30, 31, 32, 33, 34, 35, 36, 37, 38, 39, 40, 41, 42, 43, 44, 45, 46, 47, 48, 49, 50, 51, 52, 53, 54, 55, 56, 57, 58, 59, 60, 61, 62, 63, 64, 65, 66, 67, 68, 69, 70, 71, 72, 73, 74, 75] and hydride electrode materials [176, 177, 178, 179, 180, 181, 182, 183, 184, 185, 186, 187, 188], which are collected in Table 9.

---

### Electrochemical properties of hydrogen storage metals and alloys

The reversible charging and discharging of the hydrogen absorbing-desorbing electrodes has been reported in a large number of papers [91, 92, 157, 158, 159, 189, 190, 191, 192, 193, 194, 195, 196, 197, 198, 199, 200, 201, 202, 203, 204, 205, 206, 207, 208, 209, 210, 211, 212, 213, 214, 215, 216, 217, 218, 219, 220, 221, 222, 223, 224, 225, 226, 227, 228, 229, 230, 231, 232, 233, 234, 235, 236, 237, 238, 239, 240, 241, 242, 243, 244, 245]. The Pd-H system has been used as a classical model for the calculation of the physical and chemical properties of hydrides (see, for example, [209, 210, 211, 212, 213, 214] and references therein). However, a large specific gravity and a high cost were the two main reasons for searching for other hydrogen-absorbing alloys. Palladium absorbs hydrogen very easily from the gaseous as well as from the aqueous-liquid phase. Only with the palladium electrode is it possible to realize reversible hydrogen absorption-desorption (injection-extraction) at room temperature without surface corrosion. Furthermore, the electrochemical properties of palladium have been extensively examined [157, 158, 159, 189, 190, 191, 192, 193]. One of the important

**Table 9** Methods proposed for improving pretreatment of alloy and hydride electrode materials

Activation of grains in metal hydride alloy [1, 2, 3, 4, 5, 6, 7, 89, 98, 166, 167, 168, 169, 170, 171, 172, v, 173, 174, 175]	Activation of the surface of hydride electrode [176, 177, 178, 179, 180, 181, 182, 183, 184, 185, 186, 187, 188]
Coating the surface of alloy particles with powdered metals (Cu, Ni, Co, Fe, Zn, Cd), the dimensions of which are much smaller than alloy grains	Coating the electrode surface with mercury oxide (up to 2 wt%), which improves the hydrogen absorption efficiency at low temperatures
Electroless plating of the alloy particles with Cu, Ni, Pd, C or In layers	Coating of a thin Cd film on the surface of the hydrogen-occluding electrode increases about twice the specific capacity
Immersion of alloy in hot alkali solutions, when the thin porous oxide (hydroxide) layer is present on the alloy particles' surface	Fluorination of electrode to remove oxides and to form a protective barrier on the surface of the electrode
Annealing of micropowdered alloy in an oxidizing atmosphere (close to 100 °C and 100% RH) and fast cooling of the hydrogen-absorbing alloy in an atmosphere including steam. The surface of the powder particles is coated with porous oxide membrane containing OH radicals and further corrosion is restricted	Etching an anode in alkaline solutions at a sufficiently anodic potential to remove a part of surface oxides. Treating AB <sub>5</sub> electrode in alkaline solution containing H <sub>2</sub> O <sub>2</sub> to dissolve hydroxides of cobalt

problems in the study of the electrochemical behavior of palladium is the generation of electroadsorption-desorption hydrogen currents which are a few orders of magnitude higher than those of the surface processes. This problem was eliminated by Czerwiński et al. [246, 247, 248] by the use of a thin layer of palladium deposited on a neutral matrix. In this way the currents obtained for the oxidation of absorbed hydrogen are limited and controlled by the Pd electrode thickness. These types of electrodes have been called limited volume electrodes (LVEs) [249]. It was found that the hydrogen (and deuterium) sorption capacity of Pd, electrochemically measured as a H(D)/Pd ratio, depends significantly on the sweep rate in cyclic voltammetric experiments and also on the thickness of the LVE. Two different mechanisms for the hydrogen desorption reactions, namely the electrochemical oxidation and the non-electrochemical recombination step, have been postulated to take place in parallel within the Pd-LVE [250]. Experimental results have also proved the presence of a subsurface layer of absorbed hydrogen which was theoretically postulated in the literature [251, 252]. The incorporation of alkaline cations into palladium from basic solution during hydrogen electroadsorption processes was also suggested [253]. The LVE method has been applied to studies of hydrogen electroadsorption in Pd-Ni alloys [254].

Recently, attention has been paid to the improvement of the properties of the hydrogen storage alloys used as the negative electrode in nickel-hydrogen batteries. The kinetics of the electrochemical hydriding-dehydriding reactions is discussed in several articles [8, 91, 92, 194, 195, 196]. However, the results presented by various authors cannot be directly compared because of different sample preparation conditions. It was found that the activity of the metal hydride electrode depends not only on an alloy composition [7, 30, 36, 75, 85, 123, 126, 138, 197] but also on the sintering materials [153, 154, 155, 156], as well as the preparation and/or activation pretreatment of the electrode material [177, 178, 179, 180, 181, 182, 183, 184, 185,

186, 187, 188]. Only a small number of investigations have been performed on smooth alloy surfaces (e.g. [198, 199, 200]).

#### Electrode reactions

The main basic reactions which occur during charging and discharging of the metal hydride (MH) electrode in an alkaline solution can be expressed as follows: [8, 193]:

1. electroadsorption-desorption of hydrogen at the solid phase-solution:

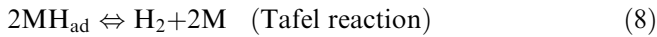


2. hydriding – dehydriding of the solid phase (solid state transfer of hydrogen):



where M = metal or multimetallic alloy forming the hydride, H<sub>ads</sub>, H<sub>α</sub> and H<sub>β</sub> denote the hydrogen atoms adsorbed on the electrode surface, in the bulk of the electrode material and in the metal hydride lattice, respectively.

On charging, the hydrogen ad-atoms are generated on the electrode surface by the electroreduction of water molecules (Eq. 5). Most of these move by diffusion into the interior of the electrode material, forming a solid solution in the host lattice (MH<sub>α</sub> phase in Eq. 6); finally, on attainment of a certain limiting concentration of hydrogen, a metal hydride (MH<sub>β</sub> phase in Eq. 7) starts to develop [1, 7, 9, 209]. Additionally, if the hydrogen penetration and incorporation into the bulk of the solid phase proceeds far slower relative to the initial charge-transfer step, then the H ad-atoms participate in chemical and/or electrochemical recombination steps (Eqs. 8 and 9), resulting in evolution of molecular hydrogen:



The Volmer-Tafel mechanism for  $\text{H}_2$  evolution has been well demonstrated on palladium and its alloys as well as on numerous hydrogen sorbing LaNi<sub>5</sub> and Ti-Zr-V-Ni based alloys [3, 7, 8, 192, 193, 194, 195, 196, 197, 198, 199, 200, 201, 202, 203, 206, 207]. The Volmer-Heyrovsky mechanism was also assumed for Ni-Mo alloys [255].

During the electrode discharge, the above reactions (Eqs. 5, 6, 7, 8, 9) run in the reverse direction. The hydrogen atoms released from the hydride phase, and/or formed at the electrode surface owing to the dissociative chemisorption of molecular hydrogen, undergo electrooxidative desorption. Any decrease in the surface concentration of H ad-atoms induces diffusion of hydrogen from the bulk of the hydride phase towards the electrode-solution interface.

Note that hydrogen evolution reduces the efficiency of the hydriding-dehydriding cycles of the MH electrodes. Therefore, it is necessary to develop such alloy materials for which the Volmer reaction and hydrogen diffusion in the bulk of the electrode material should proceed faster relative to the Tafel and/or Heyrovsky reactions.

#### Equilibrium and kinetics in the M/MH system

Electrochemical PC isotherms for hydrogen storage alloys are acquired by monitoring the equilibrium potential ( $E_{\text{MH,eq}}$ ) as a function of hydrogen content in the solid phase during the successive charge-discharge cycles. The  $E_{\text{MH,eq}}$  value of the MH electrode in alkaline solution, as measured with respect to the Hg,HgO/OH<sup>-</sup> reference electrode, is converted to equilibrium pressure of hydrogen [in the sense of cavity pressure,  $p(\text{H}_2)$ ] on the basis of the Nernst equation [7, 199, 204, 205]:

$$\begin{aligned} E_{(\text{MH,eq})} &= E^\circ(\text{H}_2\text{O}/\text{H}_2) - E^\circ(\text{Hg,HgO}/\text{OH}^-) \\ &\quad - (RT/2F)\ln[a(\text{H}_2\text{O})/a(\text{H}_2)] \\ &= E^\circ(\text{H}_2\text{O}/\text{H}_2) - E^\circ(\text{Hg,HgO}/\text{OH}^-) \\ &\quad - (RT/2F)\ln\{[a(\text{H}_2\text{O})/\gamma(\text{H}_2)] \\ &\quad \times [p(\text{H}_2)/p^\circ]\} \end{aligned} \quad (10)$$

where  $E^\circ(\text{H}_2\text{O}/\text{H}_2)$  and  $E^\circ(\text{Hg,HgO}/\text{OH}^-)$  are the standard potentials of the  $\text{H}_2\text{O}/\text{H}_2$  couple and Hg,HgO/OH<sup>-</sup> redox couples (at pH 14), respectively;  $a(\text{H}_2\text{O})$  is the activity of water,  $a(\text{H}_2)$  is the activity of hydrogen,  $\gamma(\text{H}_2)$  is the fugacity coefficient of hydrogen, and  $p^\circ$  is the standard pressure. Taking the values of  $\gamma(\text{H}_2)$  and  $a(\text{H}_2\text{O})$  for the MH electrode in 6 M KOH at  $T=293$  K under  $p=1.032 \times 10^{-5}$  N m<sup>-2</sup> [205], the relationship between  $E_{\text{MH,eq}}$  and  $p(\text{H}_2)$  is as follows [199]:

$$\begin{aligned} E_{\text{MH,eq}}(\text{vs. Hg,HgO}/\text{OH}^-) \\ = -0.9324 - 0.0291 \log[p(\text{H}_2)/p^\circ] \end{aligned} \quad (11)$$

One should notice that the PC isotherms reported for La-Ni-M and Zr-Ti-V-M (M=Mn, Cr, Cu, Ni) alloy electrodes are in good agreement with those obtained using the Sievert procedure in a solid phase-gas system [91, 92]. The equilibrium electrode potential is shifted to the positive direction for the metal hydrides of high stability and low equilibrium hydrogen pressure within the plateau region (the  $\text{MH}_\alpha$  to  $\text{MH}_\beta$  transition) of the PC isotherm. However, it becomes more negative with decreasing M-H binding energy and increasing  $p(\text{H}_2)$ . The advantage of the electrochemical technique is that it allows an evaluation of the equilibrium hydrogen pressure over a wide range from  $10^{-3}$  N m<sup>-2</sup> to  $10^7$  N m<sup>-2</sup> while using only a small amount of the charged or discharged MH material. However, at the present time, electrochemical isotherm data are still rather scarce.

The hydrogen pressure in the plateau region of the PC isotherms, directly related to the M-H interaction energy, together with the maximum hydrogen content in the metal hydride, determine the coulombic charge-discharge capacity and thus the energy stored in the MH electrode. In general it is difficult to charge an electrode material characterized by a relatively high  $p(\text{H}_2)$ , as from about  $E=-0.93$  V most of the charge is consumed in the generation of gaseous hydrogen. Only a limited hydrogen storage capacity, because of hydrogen evolution during the electrode charging, is found for intermetallic compounds and alloys forming unstable hydrides, with  $p(\text{H}_2)$  above  $5 \times 10^5$  N m<sup>-2</sup>. On the other hand, a reduced discharge capacity has been reported for electrode materials forming exceedingly stable hydrides, with  $p(\text{H}_2)$  lower than  $10^3$  N m<sup>-2</sup>. This can be explained by the oxidation of the metallic phase owing to the positive shift of the equilibrium potential of the hydrogen storage electrode. According to Iwakura and Matsuoka [3], the desirable  $p(\text{H}_2)$  value for hydride electrodes should lie in the range between  $1 \times 10^4$  N m<sup>-2</sup> and  $5 \times 10^5$  N m<sup>-2</sup>. This can be achieved by the appropriate selection of both the composition and stoichiometry of the alloy used as the electrode material.

There there has been some research on the effect of the electronic and crystallographic structure of AB<sub>5</sub> and AB<sub>2</sub> alloys on the stoichiometry and stability of the hydride phase ([69] and references therein). The amount of hydrogen absorbed in the plateau region of the PC isotherms, as well as the value of the equilibrium pressure during the  $\text{MH}_\alpha$  to  $\text{MH}_\beta$  transition, has been shown to be dependent on the density of the d states and the energy of the Fermi level in the alloy electronic structure, as well as on the unit cell parameters and the unit cell volume of the host lattice. However, in spite of considerable experimental evidence already collected, further studies are needed in order to obtain a better understanding of the various factors that influence the metal-hydrogen equilibrium

and the relative reaction rates of hydride formation and hydrogen evolution.

Apart from thermodynamic properties, an important criterion for selection of the M/MH system for practical use in electrochemical energy conversion devices (i.e. in Ni-MH batteries) is the kinetics of the hydrogen electro-sorption-desorption on the alloy/electrolyte interface and within the bulk of the solid phase (Eqs. 5, 6, 7, 8, 9). This is reflected in the value of the apparent exchange current density ( $j_0$ ) and/or activation resistance ( $R_p = (dJ/d\eta)_{\eta=0}$ ), being a measure of the catalytic activity of an alloy [3, 8, 193, 194, 197, 203, 207, 208, 217], as well as in the hydrogen diffusion coefficient ( $D$ ) and/or diffusion resistance ( $R_D$ ) which characterize the mass transport properties of the M-H electrode. Obviously, increasing the exchange current density and/or the hydrogen diffusivity increases the discharge capacity and the charge-discharge efficiency of the hydrogen storage materials in Ni-MH batteries. The same effect can be achieved by decreasing the activation enthalpy of the charge transfer reaction ( $\Delta H^*$ ). The  $\Delta H^*$  value can be directly determined from the electrochemical impedance spectra [234].

Generally, the relative rate of the individual reactions (Eqs. 5, 6, 7, 8, 9) and, consequently, the coulombic efficiency of hydrogen entry-withdrawal in a M-H system, strongly depends on the magnitude of the metal-hydrogen interaction energy. The electroreduction of water molecules (Eq. 5) becomes faster on increasing the energy of hydrogen adsorption, whereas the rate of hydrogen evolution (Eqs. 8 and/or 9) decreases. The opposite is true for the back direction of these reactions [199].

Holleck and Flanagan [208] have shown that the exchange current density ( $j_0$ ) obtained on Pd and Pd-Au electrodes was a function of hydrogen concentration in the bulk. Yayama et al. [217] noticed similar results for TiMn<sub>1.5</sub> and proposed a simple theoretical model to describe both the  $j_0$  value and the equilibrium potential ( $E_{MH,eq}$ ) as a function of the H/M ratio. More recently, this model has been used by Yang et al. [194] for the evaluation of the equilibrium between the hydrogen adsorbed on the electrode surface and the hydrogen absorbed in the bulk of the solid phase.

Table 10 summarizes the  $j_0$  values for electro-sorption-desorption of hydrogen obtained so far on intermetallic compounds and multi-metallic alloys in an alkaline medium. Unfortunately, a simple comparison of the data reported by various research groups is very difficult owing to a strong influence of the sample preparation on the degree of hydrogenation of the solid phase and, thus, on the measured values.

Presently, there is no doubt that the electrocatalytic activity of hydrogen storage alloys is influenced both by the crystallographic and electronic structure. For pure metals, a theoretical approach is possible but for the alloys only qualitative considerations have been made so far [63, 210]. A strong correlation between the stability of intermetallic compounds and their hydrides is suggested

**Table 10** Exchange current density for hydrogen sorption-desorption at hydrogen storage electrodes

Alloy	Exchange current density, $j_0$	Ref
MmB <sub>4.4</sub>	52.5 mA/g	[3]
MmB <sub>5</sub>	46.2 mA/g	[3]
MmB <sub>5.6</sub>	10 mA/g	[3]
Mm(Ni <sub>3.6</sub> Mn <sub>0.4</sub> Al <sub>0.3</sub> Co <sub>0.7</sub> ) <sub>0.88</sub>	520 mA/g	[206]
Mm(Ni <sub>3.6</sub> Mn <sub>0.4</sub> Al <sub>0.3</sub> Co <sub>0.7</sub> ) <sub>0.96</sub>	560 mA/g	[206]
Mm(Ni <sub>3.6</sub> Mn <sub>0.4</sub> Al <sub>0.3</sub> Co <sub>0.7</sub> ) <sub>1.00</sub>	600 mA/g	[206]
Mm(Ni <sub>3.6</sub> Mn <sub>0.4</sub> Al <sub>0.3</sub> Co <sub>0.7</sub> ) <sub>1.12</sub>	720 mA/g	[206]
MmNi <sub>3.5</sub> Co <sub>0.7</sub> Al <sub>0.8</sub> (Cu)	1.3 $\mu$ A/cm <sup>2</sup>	[8]
Mm <sub>0.5</sub> La <sub>0.5</sub> Ni <sub>2</sub> Co <sub>3</sub> (Cu)	0.8 $\mu$ A/cm <sup>2</sup>	[8]
MmNi <sub>5</sub> smooth surface	200 $\mu$ A/cm <sup>2</sup>	[198]
LaNi <sub>5</sub> smooth surface	316 $\mu$ A/cm <sup>2</sup>	[198]
LaNi <sub>5</sub> (PTFE)	10 $\mu$ A/cm <sup>2</sup>	[8]
LaNi <sub>5</sub> (Cu)	4 $\mu$ A/cm <sup>2</sup>	[8]
La <sub>0.8</sub> Ce <sub>0.2</sub> Ni <sub>2</sub> Co <sub>3</sub> (Cu)	4 $\mu$ A/cm <sup>2</sup>	[8]
La <sub>0.7</sub> Nb <sub>0.3</sub> Ni <sub>2.5</sub> Co <sub>2.4</sub> Cr <sub>0.1</sub> (Cu)	1.6 $\mu$ A/cm <sup>2</sup>	[8]
LaNi <sub>2.5</sub> Co <sub>2.5</sub> (Cu)	1.3 $\mu$ A/cm <sup>2</sup>	[8]
LaNi <sub>2.5</sub> Co <sub>2.4</sub> Mn <sub>0.1</sub> (Cu)	0.8 $\mu$ A/cm <sup>2</sup>	[8]
Ni smooth surface	7.9 $\mu$ A/cm <sup>2</sup>	[198]
Ni thin film (100 nm)	1.4 $\mu$ A/cm <sup>2</sup>	[203]
Ni wire	0.45 $\mu$ A/cm <sup>2</sup>	[203]
Ni (PTFE)	10 $\mu$ A/cm <sup>2</sup>	[8]
Pt smooth surface	1 mA/cm <sup>2</sup>	[198]
Pd smooth surface	126 $\mu$ A/cm <sup>2</sup>	[198]
TiMn <sub>1.5</sub> crystalline at low $c_H$	1.45 mA/cm <sup>2</sup>	[217]
TiMn <sub>1.5</sub> crystalline at high $c_H$	14.2 mA/cm <sup>2</sup>	[217]
CeCo <sub>3</sub> (PTFE)	25 $\mu$ A/cm <sup>2</sup>	[8]
CeCo <sub>2</sub> Ni (PTFE)	100 $\mu$ A/cm <sup>2</sup>	[8]
CeCoNi <sub>2</sub> (PTFE)	200 $\mu$ A/cm <sup>2</sup>	[8]
CeNi <sub>3</sub> (PTFE)	631 $\mu$ A/cm <sup>2</sup>	[8]
LaNi <sub>5</sub> thin film (200 nm)	0.58 $\mu$ A/cm <sup>2</sup>	[203]
Ni <sub>0.11</sub> Ti <sub>0.89</sub> thin film (200 nm)	2.1 $\mu$ A/cm <sup>2</sup>	[203]
Ni <sub>0.76</sub> Ti <sub>0.24</sub> thin film (150 nm)	2.6 $\mu$ A/cm <sup>2</sup>	[203]

[63, 210]. In accordance with the Engel-Brewer theory of intermetallic bond stability, Jakšić [63] has pointed out that a synergistic effect in hydrogen electro-sorption-desorption should arise by alloying metals having unoccupied d-band states with those having internally paired d-electrons. According to Ezaki et al. [210], the adsorption properties of the electrode surface can be explained by changes in the Fermi level in an alloy compared with pure metals. Nevertheless, such relationships are not always satisfactory for pure metals [210].

The charge-discharge performance of hydrogen storage electrodes may be strongly limited by transport properties of metal hydride electrodes. An evaluation of the hydrogen diffusion from the alloy surface into the lattice sites within the bulk of electrode material and/or in the back direction is a complex problem, because it is influenced both by a micro- and macrostructure of an alloy [189, 190, 191, 192, 193, 194, 195, 196, 197, 198, 199, 200, 214, 215, 216, 217, 218, 219, 220, 221, 222, 223, 224]. One has also to bear in mind that, for metal hydrides, the Fickian diffusion model might not be appropriate [216]. The diffusion of hydrogen into the bulk of electrode materials can occur in two ways, either as the random walk of a single atom (Einstein diffusion) or as a net flux in a concentration gradient (Fick's diffusion) [41].

So far, a broad scope of mass transport data have been reported only for Pd- and LaNi<sub>5</sub>-based alloys [225, 226, 227, 228, 229]. The diffusion coefficient of atomic hydrogen in the solid phase was shown to be dependent on the strength of the metal-hydrogen interaction and the hydrogen concentration in the bulk ( $c_H$ ). Wicke et al. [190] derived the thermodynamic factor  $g(\Theta_H)$ , reflecting the effect of the  $c_H$  value on the experimentally measured diffusion coefficient of hydrogen atoms in the hydride phase ( $D_H^{\text{exp}}$ ) in relation to the real diffusion coefficient ( $D_H$ ):

$$g(\Theta_H) = D_H^{\text{exp}}(\Theta_H)/D_H \quad (12)$$

where  $\Theta_H$  is defined by the ratio  $\Theta_H = c_H/c_{H,\text{max}}$  ( $c_{H,\text{max}}$  is the maximum possible concentration of hydrogen atoms in the metal and/or alloy).

Feldberg and Reilly [216] suggested a simple and straightforward relationship between the rate of hydrogen transport and the equilibrium pressure of hydrogen in the plateau region of PC isotherms. The authors developed a mathematical formalism for a synthetic isotherm, which can be relatively simply computed from the experimental isotherm. The activation energies of hydrogen diffusion estimated for LaNi<sub>5</sub> and Mg<sub>2</sub>Ni were 275 meV and 460 meV per hydrogen atom, respectively.

According to Sakamoto and Ishimaru [218], the diffusion coefficient of hydrogen in a solid solution  $\alpha$ -MH phase is not influenced by hydrogen concentration. For the metal hydride phase ( $\alpha/\beta$  and  $\beta$ ) one must take into account the hydrogen-hydrogen interaction,  $W_{H-H}$ . In the latter case, the  $D_H$  value can be evaluated according to [41]:

$$D_H = D^* \left\{ 1 + \left( \frac{W_{H-H}}{RT} \right) c_H \right\} \quad (13)$$

where  $D^*$  is the Einstein diffusion coefficient.

Some studies have been concerned with hydrogen diffusion in thin film hydrogen storage alloys [219]. Various techniques were used to determine the value of the chemical diffusion coefficients, i.e. the microelectrode technique [220], the potential-step method [221] and the optical method [222, 224], and by combining the current pulse method (Zuchner et al. [223]) with the electrochromic effect of transition metal oxides. The experimental  $D_H^{\text{exp}}$  values for some hydride-forming alloys are listed in Table 11. There are great discrepancies in results reported by various authors. For example, the reported values for the diffusion coefficient of hydrogen in LaNi<sub>5</sub> vary over three orders of magnitude at room temperature [225, 226, 227, 228, 229].

Electrochemical impedance spectroscopy and methods to study the structure of hydride electrodes

Electrochemical impedance spectroscopy (EIS) is a powerful method for investigating interface processes and electrode behavior [233, 234, 235, 236, 237, 238, 239,

**Table 11** Diffusion coefficients of atomic hydrogen in metal hydride alloys

Alloy	Diffusion coefficient (cm <sup>2</sup> /s)	Ref
LaNi <sub>5</sub>	$5 \times 10^{-6}$	[225]
LaNi <sub>5</sub>	$2.7 \times 10^{-8}$	[226]
LaNi <sub>5</sub>	$6.1 \times 10^{-9}$	[227]
LaNi <sub>5</sub>	$1 \times 10^{-6}$	[228]
LaNi <sub>5</sub>	$1 \times 10^{-10}$	[229]
FeTi	$1.8 \times 10^{-12}$	[227]
Zr <sub>36</sub> Ni <sub>64</sub>	$2.2 \times 10^{-10}$	[230]
Zr <sub>35</sub> Ni <sub>65</sub>	$1 \times 10^{-8}$ (H/M = 0.001)	[231]
Zr <sub>35</sub> Ni <sub>65</sub>	$1 \times 10^{-6}$ (H/M = 0.3)	[231]
Ti <sub>2</sub> Ni	$2.3 \times 10^{-10}$	[227]
TiMn <sub>1.5</sub>	$5 \times 10^{-11}$	[217]
LaNi <sub>4.25</sub> Al <sub>0.75</sub>	$2.97 \times 10^{-11}$	[221]
La <sub>0.65</sub> Ce <sub>0.35</sub> Ni <sub>3.55</sub>	$5.6 \times 10^{-10}$	[193]
Co <sub>0.75</sub> Mn <sub>0.4</sub> Al <sub>0.3</sub>		
MmNi <sub>4.0</sub> Mn <sub>0.75</sub> Al <sub>0.25</sub>	$7.49 \times 10^{-8}$	[41]
MmNi <sub>3.8</sub> Mn <sub>0.75</sub> Al <sub>0.5</sub> Co <sub>0.2</sub>	$4.45 \times 10^{-8}$	[41]
MmNi <sub>3.6</sub> Mn <sub>0.75</sub> Al <sub>0.75</sub> Co <sub>0.4</sub>	$4.20 \times 10^{-8}$	[41]

240, 241, 242, 243, 244, 245, 256, 257, 258]. In EIS, typically, a small sinusoidal signal is used to perturb the electrochemical system and the response of the system is observed. The frequency of the sinusoidal signal is varied in a wide range, which makes it possible to investigate processes with different time constants. Usually, the equivalent circuit method is used for the analysis of the experimental EIS data. Impedance spectroscopy is a standard technique for the investigation of electrochemical systems. However, for power sources with porous electrodes, analysis of the kinetics of the processes is more difficult, which leads to some disagreements in the interpretation of the results.

A number of authors [233, 234, 244, 245, 256] have used a five-element equivalent circuit for the characterization of metal hydride electrodes. Such an equivalent circuit was applied for the Pd/H system with the assumption that it is possible to separate the double layer capacitance from the adsorption capacitance on a flat palladium electrode [258]. To simplify the interpretation procedure, ideal capacitors were included [233]. A more realistic description of EIS data is by using dispersed capacitors and constant phase elements [242]. The use of the dispersed elements (like a constant phase element) will enlarge the number of independent parameters up to 8. At the same time, the experimental data are represented in most cases by only one semicircle with a tail at low frequencies (< 10 mHz) [236, 242, 257].

There are a lot of papers on the impedance characterization of metal hydride electrodes. Some promising results for the electrochemical behavior of these electrode materials have been obtained [233, 234, 235, 236, 237, 242, 257]. On the basis of such investigations, Kuriyama et al. [244, 245, 256] proposed, for example, that the deterioration of the metal-hydride electrode, when using a copper-coated alloy powder, was caused only by the passivation of the alloy surface. Also the performance of the electrode with an uncoated alloy was dominated by

the increase in the contact resistance. Analysis of the EIS data reveals that the kinetics of the electrode process changes with the depth of discharge. The discharge behavior of  $\text{Mg}_2\text{Ni}$ -type alloys was investigated by EIS [236, 239] and the conclusion was made that the very low discharge capacity and sluggish kinetics of unmodified  $\text{Mg}_2\text{Ni}$  in alkaline solution are caused by the presence of both a large charge-transfer resistance and a mass-transfer resistance. Additions of yttrium and aluminum to  $\text{Mg}_2\text{Ni}$  considerably reduced the hydrogen-diffusion resistance in the alloy and the charge-transfer resistance on the electrode/electrolyte interface.

The discharging process at small depths-of-discharge of  $\text{LaNi}_5$  alloys is controlled by charge transfer at the electrode/electrolyte interface [234]. The EIS of Zr-Ti-V-Ni metal hydride electrodes was investigated by Vaivars et al. [242]. He compared two alternative equivalent circuits; one included the Gerischer function [258] and the other circuit contained the charge-transfer resistance. The assumption made was that the first pair of circuit elements could be interpreted as parasitic parameters, related to the complex structure of the electrodes, like the porous structure, for example. Valoen et al. [233] associated these first elements with the contact interface between the binder and the alloy particles.

EIS is a typical in situ method, allowing real-time, step-by-step investigations of charge-discharge processes on the electrodes. During the last 15 years, a number of structural methods, typically used in external applications for end-product studies, were converted to internal in situ methods and applied also to metal hydride electrodes [259, 260, 261, 262, 263, 264, 265, 266]. Some of these methods are mentioned below.

An in situ neutron diffraction method has been applied to electrochemical cells to study the behavior of metal hydride electrode materials [262, 263, 264]. With in situ neutron diffraction measurements, the absolute values of  $x$  in the hydride alloy, i.e. the composition of the alloy charged with deuterium, can be determined for various charge-discharge states, while electrochemical methods, e.g. the coulometry of cell cycling, measures only the change in  $x$ . From in situ neutron diffraction measurements it was concluded that only the  $\alpha$  phase (low hydrogen content) is present in the low-Al-content alloy  $\text{LaNi}_{4.88}\text{Al}_{0.12}\text{D}_{1.1}$ , while both  $\alpha$  and  $\beta$  phases were present in  $\text{LaNi}_{4.4}\text{Al}_{0.6}\text{D}_{1.8}$  [263].

An in situ X-ray diffraction method has been applied to investigate the lattice expanding behavior and the degradation of hydride electrode materials and cells [261]. X-ray diffraction profiles were registered during hydriding-dehydriding of the  $\text{LaNi}_{4.8}\text{Fe}_{0.2}$  electrode. With the increase of the hydrogen content, the peak intensity of the  $\alpha$  phase decreased and that of the  $\beta$  phase increased. In the plateau region, the profiles of both phases co-exist, which indicates that a discrete lattice expansion due to the transformation from  $\alpha$  to  $\beta$  must occur. Such discrete lattice expansion, accompanying the  $\alpha$  to  $\beta$  phase transition, introduces microstrains to the crystal lattice and alloy grain cracks (degradation). It

should also be noted that the expanding behavior is maximal in the  $c$ -axis direction [261].

In situ scanning tunneling microscopy (STM) is a method which allows the imaging of the topology and surface conductivity during charging and discharging of the hydride electrode [259, 265, 266]. For in situ STM investigations, both a specific electrochemical cell and chemically stable tips were developed [267]. The volume expansion of the grains of a single metal hydride ( $\text{LaNi}_{3.5}\text{CoAl}_{0.5}$ ) was observed. Topographic and conductivity images of the  $\text{Zr}(\text{V}_{0.25}\text{Ni}_{0.75})_2$  alloy indicated two phases: one reactive with low conductivity [ $\text{Zr}(\text{V}_{0.33}\text{Ni}_{0.67})_{2.3}$ ], and the second,  $\text{Zr}_7\text{Ni}_{10}$ , with high conductivity. This leads to the conclusion that  $\text{Zr}_7\text{Ni}_{10}$  catalyzes the hydrogen absorption-desorption reactions [268]. In the  $\text{ZrV}_{1.5}\text{Ni}_{1.5}$  alloy, three different crystallographic phases were found. As indicated by in situ STM results [266], two of them were passivated, but the third, the vanadium-rich ( $\text{V}_{92}\text{Ni}_8$ ) phase, was corroded. Also, in situ laser-scanning photo-electrochemical microscopy has been applied by Yang et al. [259] to investigate the surface properties of the  $\text{AB}_5$  alloy electrode during charge-discharge processes.

#### Mathematical models of metal hydride electrodes

During the last decade, a number of researchers have modeled metal hydride electrodes [267, 268, 269, 270, 271, 272, 273, 274, 275, 276, 277]. For example, Viitanen [269] developed a model of a cylindrical  $\text{LaNi}_5$ -based hydride electrode by examining the effects of particle size, electrode porosity and conductivity. Yang et al. [276] proposed a model for the MH electrode with various geometries for alloy particles (planar, cylindrical and spherical) and concluded that the discharge performance is limited by the transition of hydrogen from the absorbed state inside the bulk of the active material to the adsorbed state on the particle surface. Heikonen et al. [270, 271, 272] considered a thick porous metal hydride electrode to simulate a continuous interrupted discharge on changing certain parameters. A mathematical model for the discharge behavior of the  $\text{Ni}(\text{OH})_2/\text{LaNi}_5$  battery was presented by Paxton and Newman [273].

Petrij et al. in their review [8] divide all the existing models of metal hydride electrodes into two groups: (1) models taking into account the diffusion of hydrogen into grains of the metal hydride [267, 276] and (2) models taking into account the diffusion throughout the bulk of the electrode material [269]. These models assume the co-existence of the  $\alpha$  (low hydrogen content) and  $\beta$  (hydrogen-rich) phases in one particle (grain) with different radii. Discharge curves are presented for the cases of low current density (hydrogen diffusion in the  $\alpha$  phase as the rate-limiting step) and of high current density (the hydrogen reaction on the catalytic Ni centers as the rate-limiting step). Also, the mechanism of “up-hill diffusion” combined with interface-controlled

**Table 12** Charge-discharge characteristics of hydrogen-absorbing alloys

Composition of alloy	Electrode preparation	Hydrogen storage capacity (theoretical) (mAh/g)	Low rate discharge capacity (mAh/g)	High rate to low rate discharge capacity	Ref
<b>Electrodes based on AB<sub>5</sub> alloy</b>					
Mm(Ni <sub>3.6</sub> Mn <sub>0.4</sub> Al <sub>0.3</sub> Co <sub>0.7</sub> ) <sub>0.88</sub>	Alloy powder + PVA (2 wt%) + porous Ni	–	246	54%	[61, 62]
Mm(Ni <sub>3.6</sub> Mn <sub>0.4</sub> Al <sub>0.3</sub> Co <sub>0.7</sub> ) <sub>0.96</sub>		272	62%		
Mm(Ni <sub>3.6</sub> Mn <sub>0.4</sub> Al <sub>0.3</sub> Co <sub>0.7</sub> ) <sub>1.00</sub>	Alloy powder + PVA (2 wt%) + porous Ni	268	268	67%	[3, 17, 41, 279]
Mm(Ni <sub>3.6</sub> Mn <sub>0.4</sub> Al <sub>0.3</sub> Co <sub>0.7</sub> ) <sub>1.12</sub>		172	172	86%	
MmNi <sub>4.8</sub> Al <sub>0.2</sub>		270 mAh/g	150	25%	
MmNi <sub>4.4</sub> Al <sub>0.6</sub>		250	250	82%	
MmNi <sub>4</sub> Al		240	240	82%	
MmNi <sub>4.2</sub> Al <sub>0.4</sub> Cr <sub>0.4</sub>		220	220	96%	
MmNi <sub>4.2</sub> Al <sub>0.4</sub> Mn <sub>0.4</sub>		270	270	64%	
MmNi <sub>4.2</sub> Al <sub>0.4</sub> Fe <sub>0.4</sub>		250	250	74%	
MmNi <sub>4.2</sub> Al <sub>0.4</sub> Co <sub>0.4</sub>		255	255	79%	
MmNi <sub>4.6</sub> Al <sub>0.4</sub>		155	155	73%	
La <sub>0.8</sub> Ce <sub>0.2</sub> Ni <sub>2</sub> Co <sub>3</sub>	Alloy + Cu (1:4)	260	253	39%	[8]
La <sub>0.8</sub> Ce <sub>0.2</sub> Ni <sub>2</sub> Co <sub>3</sub>	Alloy + PTFE	253	190	6%	
MmNi <sub>3.5</sub> Co <sub>0.7</sub> Al <sub>0.8</sub>	Alloy + Cu (1:4)	240	167	50%	
LaNi <sub>5</sub>	Alloy + Cu (1:4)	372	–	15%	[261]
LaNi <sub>5.4</sub>		360	170	25%	
LaNi <sub>4</sub> Cu		373	270	11%	
LaNi <sub>4.2</sub> Cu		360	260	62%	
LaNi <sub>4.4</sub> Cu		283	–	90%	
LaNi <sub>5</sub> Cu		198	180	98%	
Cryst. La <sub>0.8</sub> Ce <sub>0.2</sub> Ni <sub>4.75</sub> Sn <sub>0.25</sub>	Alloy + acetylene black + polymer	250	176	28%	[128]
Amorph. La <sub>0.8</sub> Ce <sub>0.2</sub> Ni <sub>4.75</sub> Sn <sub>0.25</sub>					
Cryst. La <sub>0.8</sub> Ce <sub>0.2</sub> Ni <sub>3.2</sub> CoMn <sub>0.6</sub> Al <sub>0.2</sub>		329	310	89%	
Amorph. La <sub>0.8</sub> Ce <sub>0.2</sub> Ni <sub>3.2</sub> CoMn <sub>0.6</sub> Al <sub>0.2</sub>		205	190	84%	
LaNi <sub>5</sub>	Alloy + 20 wt% TAB-3	370	171	95%	[7]
<b>Electrodes based on A<sub>2</sub>B/AB/AB<sub>2</sub> alloys</b>					
TiV <sub>4</sub>	Alloy + Ni (1:4) + PVA	852 (TiV <sub>4</sub> H <sub>8</sub> )	–	–	[104, 109, 115]
TiV <sub>4.6</sub> Ni <sub>0.4</sub>			110	–	
TiV <sub>4.4</sub> Ni <sub>0.6</sub>			350	–	
TiV <sub>4.2</sub> Ni <sub>0.8</sub>			210	–	
TiV <sub>4</sub> Ni			200	–	
ZrV <sub>0.1</sub> Mn <sub>0.9</sub> Ni-C14	Alloy powder + PVA (2 wt%)	–	140	8%	[118, 119, 280, 281, 282]
ZrV <sub>0.2</sub> Mn <sub>0.8</sub> Ni-C14			190	20%	
ZrV <sub>0.3</sub> Mn <sub>0.7</sub> Ni-C14, C15			240	34%	
ZrV <sub>0.4</sub> Mn <sub>0.6</sub> Ni-C14, C15			290	60%	
ZrV <sub>0.5</sub> Mn <sub>0.5</sub> Ni-C14, C15			280	82%	
ZrV <sub>0.6</sub> Mn <sub>0.4</sub> Ni-C14, C15			160	–	
ZrV <sub>0.8</sub> Mn <sub>0.2</sub> Ni-C15			50	–	
Ti <sub>2</sub> Ni	Alloy + 20 wt% TAB-3	–	336	97%	[227]
Ti <sub>0.26</sub> Zr <sub>0.07</sub> V <sub>0.24</sub> Mn <sub>0.20</sub> Ni <sub>0.23</sub>	Alloy + 10wt.% Ni + 10wt.% PTFE	–	295	–	[283]
Ti <sub>0.28</sub> Zr <sub>0.07</sub> V <sub>0.22</sub> Mn <sub>0.18</sub> Ni <sub>0.23</sub>			370	–	
Ti <sub>0.26</sub> Zr <sub>0.07</sub> V <sub>0.17</sub> Mn <sub>0.17</sub> Ni <sub>0.30</sub>			380	–	
Ti <sub>0.26</sub> Zr <sub>0.07</sub> V <sub>0.17</sub> Mn <sub>0.17</sub> Ni <sub>0.33</sub>			385	–	
Zr <sub>0.35</sub> Ti <sub>0.65</sub> V <sub>0.85</sub> Cr <sub>0.26</sub> Fe <sub>0.17</sub> Ni <sub>1.13</sub>	Alloy pressed between two Ni nets	–	240	–	[91]
Zr <sub>0.5</sub> Ti <sub>0.5</sub> V <sub>0.85</sub> Cr <sub>0.26</sub> Ni <sub>1.3</sub>			210	–	
Zr <sub>0.5</sub> Ti <sub>0.5</sub> V <sub>0.85</sub> Cr <sub>0.26</sub> Fe <sub>0.17</sub> Ni <sub>1.13</sub>			180	–	
Cryst. Zr <sub>36</sub> (V <sub>0.33</sub> Ni <sub>0.66</sub> ) <sub>64</sub>	Alloy pressed between two Ni screens	–	170	–	[281]
Amorph. Zr <sub>36</sub> (V <sub>0.33</sub> Ni <sub>0.66</sub> ) <sub>64</sub>			80	–	
Ti <sub>0.35</sub> Zr <sub>0.65</sub> NiV <sub>0.8</sub> Mn <sub>0.2</sub>	Alloy + Ni (1:3) + 3 wt% PTFE	–	150	27%	[90, 103]
Ti <sub>0.35</sub> Zr <sub>0.65</sub> NiV <sub>0.6</sub> Mn <sub>0.4</sub>			305	25%	
Ti <sub>0.35</sub> Zr <sub>0.65</sub> Ni <sub>1.2</sub> V <sub>0.6</sub> Mn <sub>0.2</sub>			305	52%	
Ti <sub>0.35</sub> Zr <sub>0.65</sub> Ni <sub>1.2</sub> V <sub>0.4</sub> Mn <sub>0.4</sub>			260	54%	
<b>Mg-Ni alloys</b>					
Mg <sub>2</sub> Ni	Alloy powder + Ni powder (1:4) + PVA + porous Ni, drying 120 °C, vac, p = 1200 kg/cm <sup>2</sup>	999 mAh/g	320 (303 K) 398 (343 K) 421 (363 K)	–	[236]
Mg <sub>1.9</sub> Al <sub>0.1</sub> Ni <sub>0.9</sub> Y <sub>0.1</sub>			150	70%	[239]



phase boundary movement was successfully applied to the  $\text{La}(\text{NiAl})_5\text{H}_x$  electrode to evaluate the hydrogen discharge of metal hydride electrodes [270]. In all these models it was assumed that both  $\alpha$  and  $\beta$  phases of the alloy hydrogen storage material could be characterized by constant values of the hydrogen diffusion coefficient and Fickian diffusion conditions. As mentioned already above, Feldberg and Reilly [216] predicted the electrochemical properties of metal hydride electrodes on the basis of the theory developed by Wicke et al. [190].

#### Charge-discharge performance of metal hydride electrodes

Various performance parameters of the MH electrodes, such as hydrogen storage capacity, coulombic efficiency of the hydriding-dehydriding reaction, specific power, specific energy and cycle life were investigated and compared on the basis of charge-discharge characteristics.

For example, it was established that the electrode made of  $\text{LaNi}_5$  alloy reaches maximum capacity (360 mAh/g) already in the first cycle, but the discharge capacity decreases very quickly in next cycles [278]. Such a high deterioration rate for the  $\text{LaNi}_5$  alloy electrode makes it unsuitable for use in Ni-MH batteries. However, a partial replacement of nickel with cobalt, or aluminum, increases the cycle life of the electrode. Also, Ce, Nd and Pr substitution at the La site results in improved capacity retention during cycling [5].

Among others, it was found that the discharge efficiency and, thus, the cycle life of both  $\text{AB}_5$ - and  $\text{AB}_2$ - type hydrogen storage electrodes decreases with increasing discharge current density (e.g. [279, 280, 281, 282, 283] and see Table 12). This phenomenon was explained by the depletion of atomic hydrogen from the M-H particle surface. Indeed, Kopczyk et al. [91] showed that hydrogen diffusion in the  $\text{Zr}_{0.35}\text{Ti}_{0.65}\text{V}_{0.85}\text{Cr}_{0.26}\text{Ni}_{1.3}$  and  $\text{Zr}_{0.35}\text{Ti}_{0.65}\text{V}_{0.85}\text{Cr}_{0.26}\text{Fe}_{0.17}\text{Ni}_{1.13}$  alloys was the controlling step at a deep depth of the electrode discharge. The diffusion resistance of the discharged electrode material was higher by a factor of about 10 than that for the charged electrodes. Both lower hydrogen storage capacity and cycling efficiency was found with increasing Zr content in an alloy. Züttel et al. [284] pointed out that some alloy grains in the porous MH electrode cannot be discharged owing to poor electrical contact and thus a high internal resistance of the electrode material. On the other hand, it is well known that the activation of an electrode material towards the hydrogen adsorption-desorption reaction becomes easier at higher charge-discharge current densities [276].

One of the serious problems of Ni-MH batteries is corrosion and degradation of the MH electrode. Hydrogen-absorbing alloys are formed from various metallic constituents and each of them has its own characteristic oxidation potential in an alkaline electrolyte. For example, it was shown by Willems et al. [1, 42,

43] that La reacts with water, giving hydroxide or oxide at potentials of about  $-2.0$  V with respect to the reversible hydrogen electrode. The addition of relatively small quantities of Al, Cr or Si can protect the underlying metal from further oxidation. According to the results of Ikoma et al. [52], the corrosion resistance of the negative electrode can be increased by improving the crystallinity of the alloy (in sequences of rapid cooling and heating), as well as by increasing the specific surface area of the electrode material. The data on corrosion of the  $\text{AB}_5$ - and  $\text{AB}_2$ -type alloys and alloy hydride electrodes can be found in several papers (i.e. [33, 42, 43, 44, 45, 52, 284, 285, 286, 287, 288, 289, 290, 291, 292, 293, 294, 295, 296, 297, 298]).

In conclusion, one can say that the development of hydrogen storage alloys with high capacity and catalytic properties has a key importance for further improvement of Ni-MH battery performance.

**Acknowledgements** Financial support for this work from the State Committee for Scientific Research of Poland (KBN grant no. 8T10A 02510) is gratefully acknowledged.

#### References

1. Willems JG (1984) Philips J Res 39:1
2. Iwakura C, Sakai T (1989) J Hydrogen Energy Syst Soc Jpn 11(2):13
3. Iwakura C, Matsuoka M (1991) Prog Batteries Battery Mater 10:81
4. Fetcenko MA, Venkatesan S, Ovshinsky SR (1992) In: Corrigan DA, Srinivasan S (eds) Proceedings of a symposium on hydrogen storage materials, batteries and electrochemistry, vol 92-5. The Electrochemical Society, Pennington, NJ, pp 141-167
5. Sakai T, Muta K, Miyamura H, Kuriyama N, Ishikawa H, (1992) In: Corrigan DA, Srinivasan S (eds) Proceedings of a symposium on hydrogen storage materials, batteries and electrochemistry, vol 92-5. The Electrochemical Society, Pennington, NJ, pp 59-91
6. Berndt D (1994) Maintenance-free batteries. A handbook of battery technology. Wiley, New York, p 362
7. Sakai T, Matsuoka M, Iwakura C (1995) In: Gschneidner KA, Eyring L (eds) Handbook on the physics and chemistry of rare earths, vol. 21. Elsevier, Amsterdam, pp 135-180
8. Petrii OA, Vasina SYa, Korobov II (1996) Usp Khim 65:195
9. Solonin JM, Kolomijec LL, Skorochod BB (1993) Mater Ukr Acad Sci 93
10. Dantzer P (1997) In: Wipf H (ed) Topics in applied physics, vol 73. Springer, Berlin Heidelberg New York, pp 279-340
11. Dhar SK, Ovshinsky SR, Gifford PR, Corrigan DA, Fetcenko MA, Venkatesan S (1997) J Power Sources 65:1
12. Wang QD, Chen CP, Lei YQ (1997) J Alloys Compd 253: 6294
13. Uehara I, Sakai T, Ishikawa H (1997) J Alloys Compd 253:635
14. Nagarajan GS, Van Zee JW (1998) J Power Sources 70:173
15. Anani A, Visintin A, Petrov K, Srinivasan S (1994) J Power Sources 47:261
16. Kleperis J (1993) Review: metal hydride electrodes (in patents and papers). Stockholm University, Sweden, p 85
17. Withers JC, Loutfy RO, Lowe TP (1997) Fullerene Sci Technol 5:1
18. Brunning HACM, Westendorp FF, van Vucht JHN, Zijlstra H (Philips' Gloeilampenfabrieken) (1969) Ger Patent A-2,003,749

19. Beccu K, Siegert R (Batelle Memorial Institute International Division) (1968) Fr Patent 1,565,808
20. Oswin HG (Leesona Corporation) (1963) US Patent 3,092,517
21. Wolf EV (Electric Storage Battery Company) (1965) US Patent 3,202,544
22. Lindholm I (Allmanna Svenska Elektriska Aktiebolaget) (1966) US Patent 3,262,816
23. Beccu K (Batelle Memorial Institute) (1972) US Patent 3,669,745
24. Beccu K (Batelle Memorial Institute) (1974) US Patent 3,824,131
25. Jung M, Kroeger HH (Varta Aktiengesellschaft) (1968) US Patent 3,409,474
26. Yartus VA, Burnasheva VV, Semenenko KN, Fadeeva NV, Solov'ev SP (1982) Int J Hydrogen Energy 7:957
27. Dilworth LR, Wunderlin WJ (Allis-Chalmers Manufacturing Company) (1968) US Patent 3,405,008
28. Dilworth LR (Allis-Chalmers Manufacturing Company) (1968) US Patent 3,405,009
29. Dunlop JD, Stockel J (Communications Satellite Corporation) (1978) US Patent 4,112,199
30. Notten PHL, Hokkeling P (1991) J Electrochem Soc 138:1877
31. Bernd F (1992) Product information. Gesellschaft für Elektrometallurgie, Nürnberg
32. Bridger NJ, Markin TL (UK Atomic Energy Authority) (1976) GB Patent A-1,546,613
33. Heuts JF, Willems JG (Philips' Gloeilampenfabrieken) (1987) Eur Patent A-0 251 384 A1
34. Yagasaki E, Kanda M, Mitsuyasu K, Sato Y (Toshiba) (1986) Eur Patent A-0 206 776 A2
35. Chen J, Dou SX, Liu HK (1996) J Power Sources 63:267
36. Boter PA (Philips Corporation) (1977) US Patent 4,048,407
37. Adzic GD, Johnson JR, Mukerjee S, Mcbreen J, Reilly JJ (1997) J Alloys Compd 253:579
38. Cocciantelli JM, Bernard P, Fernandez S, Atkin J (1997) J Alloys Compd 253:642
39. Züttel A, Chartouni D, Gross K, Spatz P, Bachler M, Lichtenberg F, Folzer A (1997) J Alloys Compd 253:626
40. Hu WK, Lee H, Kim DM, Jeon SW, Lee JY (1998) J Alloys Compd 268:261
41. Iwakura C, Fukuda K, Senoh H, Inoue H, Matsuoka M, Yamamoto Y (1998) Electrochim Acta 43:2041
42. Willems JJG, van Beek JR, Buschow KH (Philips' Gloeilampenfabrieken) (1984) Eur Patent A-0 142 878 A1
43. Willems JJG, van Beek JRG, Kurt HJ (1984) US Patent 4,487,817
44. Witham C, Hightower A, Fultz B, Ratnakumar BV, Bowman RC (1997) J Electrochem Soc 144:3758
45. Heuts JJFG, Willems JJGSA (Philips' Gloeilampenfabrieken) (1987) US Patent 4,699,856
46. Percheron-Guegan A, Achard J-C, Bronoe G, Sarradin J (Agence Nationale de Valorisation de la Recherche) (1977) Fr Patent A-2,382,774
47. Percheron-Guegan A, Achard J-C, Bronoe G, Sarradin J (Agence Nationale de Valorisation de la Recherche) (1987) Fr Patent A-2,399,484
48. Percheron-Guegan A, Achard CJ, Lories J, Bonnemay M, Bronoe G, Sarradin J, Schlapbach L (Agence Nationale de Valorisation de la Recherche) (1978) US Patent 4,107,405
49. Percheron-Guegan A, Achard JC, Bronoe G, Sarradin J (Agence Nationale de Valorisation de la Recherche) (1986) US Patent 4,609,599
50. Kanda M, Sato Y (Toshiba) (1984) Eur Patent A-0 149 846 A1
51. Mitsuyasu K, Kanda M, Takeno K, Kochiwa K (Toshiba) (1988) Eur Patent A-0 284 063 A1
52. Ikoma M, Kawano H, Matsumoto I, Yanagihara N (Matsushita Electric) (1987) Eur Patent A-0 271 043
53. Ikoma M, Ito Y, Yuasa K, Matsumoto I, Hino T (Matsushita Electric) (1989) Eur Patent A-0 384 945 A1
54. Ikoma M, Kawano H, Takahashi O, Matsumoto I, Ikeyama M (Matsushita Electric) (1989) Eur Patent A-0 383 991 A2
55. Ikoma M, Kawano H, Matsumoto I, Yanagihara N (Matsushita Electric) (1989) US Patent 4,837,119
56. Ikoma M, et al (Matsushita Electric) (1990) US Patent 4,925,748
57. Ikoma M, Kawano H, Ito Y, Matsumoto I (Matsushita Electric) (1990) US Patent 4,935,318
58. Ikoma MY, Ito Y, Matsumoto I, Ogawa H (1988) Extended abstracts presented at the meeting of the Electrochemical Society, no. 85, Chicago, p 174
59. Gamo T, Moriwaki Y, Iwaki T (Matsushita Electric) (1988) Eur Patent A-0 293 660 A2
60. Gamo T, Iwaki T, Shintani A (Matsushita Electric) (1990) Eur Patent A-0 413 029 A1
61. Iwakura C, Miyamoto M, Inoue H, Matsuoka M, Fukumoto Y (1997) J Alloys Compd 259:129
62. Iwakura C, Miyamoto M, Inoue H, Matsuoka M, Fukumoto Y (1997) J Alloys Compd 259:132
63. Jakšić MM (1984) Electrochim Acta 29:1539
64. Heuts JJFG, Frens G (Philips' Gloeilampenfabrieken) (1987) US Patent 4,702,978
65. Villars P, Calvert LD (1985) Pearson's handbook of crystallographic data for intermetallic phases, vols 1-3. American Society for Metals, Metals Park, Ohio
66. Percheron-Guegan A, Welter J-M (1988) In: Schlapbach L (ed) Topics in applied physics, vol. 63. Springer, Berlin Heidelberg New York, pp 11-48
67. Mohri M (Sharp) (1985) Eur Patent A-0 156 241 A2
68. Thona DJ, Perepezko JH (1995) J Alloys Compd 224:330
69. Wójcik G, Kopczyk M, Drulis H, Beltowska-Brzezinska M (1995) Wiad Chem 49:285
70. Venkatesan S, Reichman B, Fetcenko MA (Energy Conversion Devices) (1987) Eur Patent A-0 273 624 A2
71. Reichman B, Venkatesan S, Fetcenko MA, Jeffries K, Stahl S, Bennett C (Energy Conversion Devices) (1987) Eur Patent A-0 273 625 A2
72. Wolff M, Fetcenko MA, Nuss MA, Lijoi AL (Energy Conversion Devices) (1988) Eur Patent A-0 347 507 A1
73. Fetcenko MA (Energy Conversion Devices) (1989) Eur Patent A-0 360 203
74. Fetcenko MA (Energy Conversion Devices) (1990) Eur Patent A-0 410 935
75. Sapru K, Hong K, Fetcenko M, Venkatesan S (Energy Conversion Devices) (1985) US Patent 4,551,400
76. Sapru K, Reichman B, Reger A, Ovshinsky SR (Energy Conversion Devices) (1986) US Patent 4,623,597
77. Magnuson G, Wolff M, Lev S, Jeffries K, Mapes S (Energy Conversion Devices) (1987) US Patent 4,670,214
78. Reichman B, Venkatesan S, Fetcenko MA, Jeffries K, Stahl S, Bennett C (Energy Conversion Devices) (1987) US Patent 4,716,088
79. Venkatesan S, Reichman B, Fetcenko MA (Energy Conversion Devices) (1988) US Patent 4,728,586
80. Fetcenko MA, Kaatz T, Sumner SP, LaRocca J (Energy Conversion Devices) (1990) US Patent 4,893,756
81. Wolf M, Nuss MA, Fetcenko MA, Lijoi AL, Sumner SP, LaRocca J, Kaatz T (Energy Conversion Devices) (1990) US Patent 4,915,898
82. Fetcenko MA, Sumner SA, LaRocca J (Energy Conversion Devices) (1990) US Patent 4,948,423
83. Furukawa N, Inoue K, Nogami M, Kameoka S, Tadokoro M (Sanyo Electric) (1991) US Patent 5,008,104
84. Sapru K, Hong K, Venkatesan S, Fetcenko M (Ovonic Battery) (1985) Eur Patent A-0 161 075 A2
85. Fetcenko MA (1991) (Energy Conversion Devices) (1988) US Patent 5,002,730
86. Fetcenko MA, Venkatesan S, Hong KC, Reichman B (1988) J Power Sources 12:411
87. Fetcenko MA, Venkatesan S (1990) Prog Batteries Solar Cells 9:259
88. Zoitos BK, Hudson DL, Bennett PD, Puglisi VJ (1992) In: Proceedings of a symposium on hydrogen storage materials,

- batteries and electrochemistry, vol 92-5. The Electrochemical Society, Pennington, NJ, pp 168–178
89. Xan DY, Sandrock G, Suda S (1995) *J Alloys Compd* 223:32
  90. Yang HW, Jeng SN, Wang YY, Wan CC (1995) *J Alloys Compd* 227:69
  91. Kopczyk M, Wójcik G, Mlynarek G, Sierczynska A, Beltowska-Brzezinska M (1996) *J Appl Electrochem* 26:639
  92. Wójcik G, Kopczyk M, Mlynarek G, Majchrzycki W, Beltowska-Brzezinska M (1996) *J Power Sources* 58:73
  93. Chartouni D, Züttel A, Nutzenadel C, Schlapbach L, Cheng SA, Lei YQ, Liu H, Wang QD, Zhang JQ, Cao CN (1997) *J Appl Electrochem* 27:1307
  94. Deying S, Xueping G, Yunshi Z, Jie Y, Panwen S (1994) *J Alloys Compd* 206:43
  95. Xueping G, Deying S, Yunshi Z, Genshi W, Panwen S (1995) *J Alloys Compd* 223:77
  96. Ming Au, Pourariam F, Simizu S, Sankar SG, Zhang L (1995) *J Alloys Compd* 223:1
  97. Züttel A, Meli F, Schlapbach L (1994) *J Alloys Compd* 203:235
  98. Ohta M, Nakano H, Wakao S, Sawa H (1989) *Z Phys Chem NF* 164:1527
  99. Reichman B, Venkatesan S, Fetcenko MA, Jeffries K, Stahl S, Magnuson D, Bennett C, Summer S (1987) US Patent 4,716,088
  100. Fetcenko MA, Ovshinsky SR (1994) US Patent 5,330,861
  101. Miyamura H, Sakai T, Kuriyama N, Oguro K, Kato A, Ishikawa H (1992) In: *Proceedings of a symposium on hydrogen storage materials, batteries and electrochemistry, vol 92-5. The Electrochemical Society, Pennington, NJ, pp 179–198*
  102. Huot J, Akiba E, Ogura T, Ishido Y (1995) *J Alloys Compd* 218:101
  103. Yang XG, Lei YQ, Zhang WK, Zhu GM, Wang QD (1996) *J Alloys Compd* 243:151
  104. Tsukahara M, Takahashi K, Mishima T, Isomura A, Sakai T (1996) *J Alloys Compd* 245:59
  105. Sun DL, Latroche M (1997) *J Alloys Compd* 248:215
  106. Yamashita I, Tanaka H, Takeshita H, Kuriyama N, Sakai T, Uehara I (1997) *J Alloys Compd* 253:238
  107. Bououdina M, Menier P, Soubeyrou JL, Fruchart D (1997) *J Alloys Compd* 253:302
  108. Joubert JM, Sun DL, Latroche M, Percheron-Guegan A (1997) *J Alloys Compd* 253:564
  109. Tsukahara M, Takahashi K, Mishima T, Isomura A, Sakai T (1997) *J Alloys Compd* 253:583
  110. Züttel A, Chartouni D, Gross K, Bachler M, Schlapbach L (1997) *J Alloys Compd* 253:587
  111. Nakano H, Wakao S, Shimizu T (1997) *J Alloys Compd* 253:609
  112. Chen J, Dou SX, Liu HK (1997) *J Alloys Compd* 256:40
  113. Lee SF, Wang YY, Wan CC (1997) *J Power Sources* 66:165
  114. Liu WH, Wu HQ, Lei YQ, Wang QD, Wu J (1997) *J Alloys Compd* 261:289
  115. Bernauer O, Töpler J, Noréus D, Hempelmann R, Richter D, (1989) *Int J Hydrogen Energy* 14:187
  116. Doi H, Yabuki R (Mitsubishi Metal) (1990) US Patent 4,898,794
  117. Doi H, Yabuki R (Mitsubishi Metal) (1991) US Patent 4,983,474
  118. Kim SR, Lee, J-Y (1994) *J Alloys Compd* 210:109
  119. Kim SR, Lee KY, Lee JY (1995) *J Alloys Compd* 223:22
  120. Lee HH, Lee KY, Lee JY (1997) *J Alloys Compd* 253:601
  121. Hong K (Gambler) (1991) US Patent 5,006,328
  122. Ovshinsky SR, Fetcenko MA (1993) *Ross J Sci* 260:176
  123. Osawa E (1970) *Kagaku* 25:854
  124. Kroto HW, Heath JR, O'Brien SC, Curl RF, Smalley RE (1985) *Nature* 318:162
  125. Saprú K, Reichman B, Reger A, Ovshinsky SR (Energy Conversion Devices) (1983) GB Patent A-2,119,561
  126. Keem JE, Bergeron RC, Custer RC, McCallum RW (Energy Conversion Devices) (1987) US Patent 4,637,967
  127. Grasselli RK, Harris JH, Henderson RS, Tenhover MA (Standard Oil) (1990) US Patent 4,923,770
  128. Lim HS, Zelter GR, Allison DU, Haun RE (1997) *J Power Sources* 66:101
  129. Bowman RC, Witham C, Fultz B, Ratnakumar BV, Ellis TW, Anderson IE (1997) *J Alloys Compd* 253:613
  130. Kronberger H (1997) *J Alloys Compd* 253:87
  131. Li CJ, Wang XL, Wang CY (1998) *J Alloys Compd* 266:300
  132. Li C, Wang X, Li X, Wang C (1998) *Electrochim Acta* 43:1839
  133. Higashiyama N, Matsuura Y, Nakamura H, Kimoto M, Nogami M, Yonezu I, Nishio K (1997) *J Alloys Compd* 253:648
  134. Sakai T, Yoshinaga H, Miyamura H, Kuriyama N, Ishikawa H, Uehara I (1993) *J Alloys Compd* 192:182
  135. Li Y, Cheng Y-T (1995) *J Alloys Compd* 223:6
  136. Ovshinsky SR, Fetcenko MA (Ovonic Battery) (1996) US Patent 5,506,069
  137. Sun D, Lei Y, Liu W, Jiang J, Wu J, Wang O (1995) *J Alloys Compd* 231:621
  138. Chen Y, Williams JS (1995) *J Alloys Compd* 217:181
  139. Imamura H, Sakasai N, Fujinaga T (1997) *J Alloys Compd* 253:34
  140. Sun D, Latroche M, Percheron-Guegan A (1997) *J Alloys Compd* 257:302
  141. Nohara S, Inoue H, Fukumoto Y, Iwakura C (1997) *J Alloys Compd* 259:183
  142. Liu W, Lei Y, Sun D, Wu J, Wang Q (1996) *J Power Sources* 58:243
  143. Jung CB, Lee KS (1997) *J Alloys Compd* 253:605
  144. Chen J, Dou SX, Liu HK (1997) *J Alloys Compd* 248:146
  145. Liu WH, Wu HQ, Lei YQ, Wang QD, Wu J (1997) *J Alloys Compd* 252:234
  146. Lenain C, Aymard L, Salverdisma F, Leriche JB, Chabre Y, Tarascon JM (1997) *Solid State Ionics* 104:237
  147. Jung CB, Kim JH, Lee KS (1997) *Nanostruct Mater* 8:1093
  148. Kleperis J, Vaivars G, Vitins A, Lulis A, Galkin A (1996) In: Barsukov V, Beck F (eds) *New promising electrochemical systems for rechargeable batteries. (NATO ASI series 3, vol 6) Kluwer, Dordrecht, pp 285–302*
  149. Vaskelis A, Juskenas R, Jaciauskiene J (1998) *Electrochim Acta* 43:1061
  150. Juskenas R, Selskis A, Kadzizauskiene V (1998) *Electrochim Acta* 43:1903
  151. Philips Electronic (1975) GB Patent A-1,463,248
  152. Yoshinaga H, Wada M, Sakai T, Miyamura H, Kuriyama N, Uehara I (1997) *J Alloys Compd* 253:665
  153. Züttel A, Meli F, Schlapbach L (1994) *J Alloys Compd* 206:31
  154. Liu BH, Jung JH, Lee KY, Lee JY (1996) *J Alloys Compd* 245:132
  155. Züttel A, Meli F, Schlapbach L (1995) *J Alloys Compd* 221:207
  156. Heikonen JM, Ploehn HJ, White RE (1998) *J Electrochem Soc* 145:1840
  157. Baranowski B, Smialowski (1959) *Bull Acad Pol Sci Ser Sci Chim* 7:663
  158. Baranowski B (1959) *Bull Acad Pol Sci Ser Sci Chim* 7:897
  159. Baranowski B (1959) *Bull Acad Pol Sc Ser Sci Chim* 7:907
  160. Wójcik G, Kopczyk M, Kleperis J, Mlynarek G, Majchrzycki W, Vitins G, Lulis A, Beltowska-Brezinska M (1996) Abstracts, international symposium on metal hydrogen systems: fundamentals and applications, Les Diablerets, Switzerland, p 124
  161. Kleperis J, Lulis A, Vaivars G, Kopczyk M, Wójcik G, Mlynarek G, Majchrzycki W (1998) Proceedings of the VIIth international Baltic conference on materials engineering, Latvia, pp 46–50
  162. Kleperis J, Lulis A, Vitins G, Beltowska-Brezinska M, Kopczyk M, Wójcik G, Mlynarek G, Majchrzycki W (1996) Abstracts, international symposium on metal hydrogen systems: fundamentals and applications, Les Diablerets, Switzerland, p 122

163. Endoh E, Otuma H, Morimota T, Oda Y (1987) *Int J Hydrogen Energy* 12:473
164. Choquette Y, Menard H, Brossard L (1989) *Int J Hydrogen Energy* 14: 637
165. Yoshida N, Morimoto T (1994) *Electrochim Acta* 39:1733
166. Jung JH, Lee HH, Kim DM, Jang KJ, Lee JY (1998) *J Alloys Compd* 266:266
167. Jenq SN, Yang HW, Wang YY, Wan CC (1997) *Mater Chem Phys* 48:10
168. Lim HS, Zelter GR (1997) *J Power Sources* 66:97
169. Jung JH, Liu BH, Lee JY (1998) *J Alloys Compd* 264:306
170. Liu FJ, Sandrock G, Suda S (1994) *Z Phys Chem* 183:163
171. Tsukahara M, Takahashi K, Mishima T, Isomura A, Sakai T (1996) *J Alloys Compd* 243:133
172. Chen J, Bradhurst DH, Dou SX, Liu HK (1998) *J Alloys Compd* 265:281
173. Huot J, Bouaricha S, Boily S, Dodelet JP, Guay D, Schulz R (1998) *J Alloys Compd* 266:307
174. Li CH, Wang XL, Wu JM, Wang CY (1998) *J Power Sources* 70:106
175. Jung CB, Kim JH, Lee KS (1998) *J Alloys Compd* 267:265
176. Liu BH, Lee JY (1997) *J Alloys Compd* 255:43
177. Sun YM, Iwata K, Chiba S, Matsuyama Y, Suda S (1997) *J Alloys Compd* 253:520
178. Sakashita M, Li ZP, Suda S (1997) *J Alloys Compd* 253:500
179. Jung JH, Lee HH, Kim DM, Liu BH, Lee KY, Lee JY (1997) *J Alloys Compd* 253:652
180. Cheng SA, Lei YQ, Leng YJ, Wang QD (1998) *J Alloys Compd* 264:104
181. Zheng G, Popov BN, White RE (1998) *J Appl Electrochem* 28:381
182. Jung JH, Lee SM, Kim DM, Jang KJ, Lee JY (1998) *J Alloys Compd* 266:271
183. Wang CS, Lei YQ, Wang QD (1998) *J Power Sources* 70:222
184. Boter PA (Philips) (1977) US Patent 4,004,943
185. Sakai T, et al. (Japan Agency of Industrial Science and Technology) (1990) Eur Patent A-0 417 697 A2
186. Kuriyama N, Sakai T, Miyamura H, Tanaka H, Takeshita HT, Uehara I (1997) *J Alloys Compd* 253:598
187. Kuriyama N, Sakai T, Miyamura H, Tanaka H, Uehara I, Meli F, Schlapbach L (1996) *J Alloys Compd* 238:128
188. Kim SR, Lee J-Y, Park H-H (1994) *J Alloys Compd* 205:225
189. Baranowski B, Wisniewski (1966) *Bull Acad Polon Sci Ser Sci Chim* 14:273
190. Wicke E, Brodowsky H, Züchner H (1978) In: Alefeld G, Völkl J (eds) *Hydrogen in metals II*. Springer, Berlin Heidelberg New York, p 73
191. Yang T-H, Pyun SI (1996) *Electrochim Acta* 41:843
192. Mueller M, Blackledge JP, Libowitz GG (1968) *Metal hydrides*. Academic Press, New York, p 633
193. Popov BN, Zheng G, White RE (1996) *J Appl Electrochem* 26:603
194. Yang QM, Ciureanu M, Ryan DH, Ström-Olsen JO (1995) *Electrochim Acta* 40:1921
195. Ciureanu M, Yang QM, Ryan DH, Ström-Olsen JO (1994) In: Bennet PD, Sakai T (eds) *Proceedings of a symposium on hydrogen and metal hydride batteries*, vol 94-27. The Electrochemical Society, Pennington, NJ, pp 124-135
196. Iwakura C, Miyamoto M, Inoue H, Matsuoka M, Fukumoto Y (1995) *J Alloys Compd* 231:558
197. Machida K, Enyo M, Adachi G, Sakaguchi H, Shiokawa J (1986) *Bull Chem Soc Jpn* 59:925
198. Kitamura T, Iwakura C, Tamura H (1982) *Electrochim Acta* 27:729
199. Enyo M (1994) *Electrochim Acta* 39:1715
200. Wakao S, Yonemura Y (1983) *J Less-Common Met* 89:481
201. Petrii OA, Semenko KN, Korobov II, Vasina SYa, Kovrignina IV, Burnasheva VV (1987) *J Less-Common Met* 136:121
202. Tamura H, Iwakura C, Kitamura T (1983) *J Less-Common Met* 89:567
203. Machida K, Enyo M, Adachi G, Shiokawa J (1984) *Electrochim Acta* 29:807
204. Kitamura T, Iwakura C, Tamura H (1982) *Electrochim Acta* 27:1723
205. Balej J (1985) *Int J Hydrogen Energy* 10:365
206. Fukumoto Y, Miyamoto M, Matsuoka M, Iwakura C (1995) *Electrochim Acta* 40:845
207. Bittner HF, Badcock CC (1983) *J Electrochem Soc* 130:193C
208. Holleck GL, Flanagan TB (1969) *J Phys Chem* 73:285
209. Lewis FA (1967) *The palladium hydrogen system*. Academic Press, New York
210. Ezaki H, Morinaga M, Watanabe S (1993) *Electrochim Acta* 38:557
211. Sokolskii DV, Sokolskaya AM (1970) *Metally-katalizatory Hydrogenizatsii (in Russian)*. Nauka, Alma-Ata
212. Sokolskii, Zakumbaieva GD (1973) *Adsorocja i Kataliz na Metallach VIII, Gruppy w Rastworach (in Russian)*. Nauka, Alma-Ata
213. Woods R (1976) In: Bard AJ (ed) *Electroanalytical chemistry*, vol. 9. Dekker, New York, pp 1-162
214. Stalinski B, Terpilowski J (1987) *Wodor i wodorki (in Polish)*. WNT, Warsaw
215. Holleck GL, Flanagan TB (1969) *J Phys Chem* 73:285
216. Feldberg SW, Reilly JJ (1997) *J Electrochem Soc* 144:4260
217. Yayama H, Hirakawa K, Tomokiyo A (1986) *Jpn J Appl Phys* 25:739
218. Sakamoto Y, Ishimaru N (1994) *Z Phys Chem* 183:246
219. Zhou Z, Huang J, Hu W, Yao F, Zhang Y (1995) *J Alloys Compd* 231:297
220. Nishina T, Ura H, Uchida I (1997) *J Electrochem Soc* 144:1273
221. Krapivnyi NG (1982) *Elektrokhimiya* 18:1174
222. Kleperis J, Takeris S, Lulis A, Stradins J (1984) *Phys Status Solidi A* 81:K17
223. Zuchner H, Rauf T, Hempelmann R (1991) *J Less-Common Met* 611:172
224. Kleperis J, Rodionov A, Lulis A (1992) *Sov Electrochem* 28(10C):1186
225. Zheng G, Popov BN, White RE (1995) *J Electrochem Soc* 142:2695
226. Khodosov E, Linnik A, Kobsenko G, Ivanchenko V (1977) In: *Proceedings of the 2nd international congress on hydrogen in metals*, Paris. Pergamon Press, Oxford, paper 1D10
227. Reilly JJ, Wiswall RH (1974) *Inorg Chem* 13:218
228. Lebsanft E, Richter D, Topler JM (1979) *Z Phys Chem NF* 116:175
229. Fischer P, Furrer A, Busch G, Schlapbach L (1977) *Helv Phys Acta* 50:421
230. Van Rijswijk MHJ (1978) In: Anderesen AF, Maeland AJ (eds) *Hydrides for energy storage*. Pergamon Press, Oxford, p 261
231. Kirchheim R, Kieninger W, Huang XY, Filipek SM, Rush J, Udovic T (1991) *J Less-Common Met* 172:880
232. Ciureanu M, Moroz D, Ducharme R, Ryan DH, Strom-Olsen JO (1994) *Z Phys Chem NF* 183:365
233. Valoen LQ, Sunde S, Tunold R (1997) *J Alloys Compd* 253:656
234. Yang TH, Pyun SI (1996) *J Power Sources* 62:175
235. Kumar VG, Munichandraiah N, Shukla AK (1996) *J Power Sources* 63:203
236. Cui N, Luan B, Liu HK, Dou SX (1996) *J Power Sources* 63:209
237. Leng YJ (1997) *J Electrochem Soc* 144:2941
238. Zhang W, Srinivasan S (1997) *J Electrochem Soc* 144:2942
239. Cui N, Luo JL (1998) *J Alloys Compd* 265:305
240. Wang CS (1998) *J Electrochem Soc* 145:1801
241. Leng Y, Zhang J, Cheng S, Cao C, Ye Z (1998) *Electrochim Acta* 43:1945
242. Vaivars G, Kleperis J, Mlynarek G, Scierczynska A, Wojcik G, Kopezik M (1999) *Proceedings of the 5th international microsymposium on electrochemical impedance analysis, Balatonfoldvar, Hungary*, p 39
243. Boukamp BA (1986) *Solid State Ionics* 20:31

244. Kuriyama N, Sakai T, Miyamura H, Uehara I, Ishikawa H (1993) *J Alloys Compd* 202:183
245. Kuriyama N, Sakai T, Miyamura H, Uehara I, Ishikawa H (1993) *J Alloys Compd* 192:161
246. Czerwiński A, Marassi R, Zamponi S (1991) *Electroanal J Chem* 316:211
247. Czerwiński A, Marassi R (1992) *Electroanal J Chem* 322:373
248. Czerwiński A (1995) *Pol J Chem* 69:699
249. Czerwiński A, Kiersztyn I, Frydrych J (1996) *Anal Lett* 29:2549
250. Czerwiński A, Maruszczak G, Żelazowska M (1993) *Pol J Chem* 67:2037
251. Breiter MW (1979) *Electroanal J Chem* 109:253
252. Bucur RV, Bota F (1982) *Electrochim Acta* 27:521
253. Czerwiński A, Czauderna M, Maruszczak G, Kiersztyn I, Marassi R, Zamponi S (1997) *Electrochim Acta* 42:81
254. Grdeń M, Czerwiński A, Golimowski J, Bulska E, Krasnodębska-Ostrega B, Marassi R, Zamponi S (1999) *J Electroanal Chem* 460:30
255. Lasia A (1993) *Electrochemistry* 2:239
256. Kuriyama N, Sakai T, Miyamura H, Uehara I, Ishikawa H (1992) *J Electrochem Soc* 139:L72
257. Bundy K, Karlsson M, Lindberg G, Lundqvist A (1998) *J Power Sources* 72:118
258. Breiter MW (1978) *Z Phys Chem* 112:183
259. Yang Y, Li J, Nan JM, Lin ZG (1997) *J Power Sources* 65:15
260. Pyun SI, Han JN, Yang TH (1997) *J Power Sources* 65:9
261. Notten PHL, Daams JLC, Einerhand REF (1994) *J Alloys Compd* 210:233
262. Latroche M, Percheron-Guegan A, Chabre Y, Poinsignon C, Pannetier J (1992) *J Alloys Compd* 189:59
263. Latroche M, Percheron-Guegan A, Chabre Y, Bouet J, Pannetier J, Ressouche E (1995) *J Alloys Compd* 231:537
264. Peng W, Redey L, Jansen AN, Vissers DR, Myles KM, Carpenter JM, Richardson JW, Burr GL, Selman JR (1997) *J Electrochem Soc* 144:3836
265. Chartouni D, Zuttel A, Nutzenadel C, Schlapbach L (1997) *J Alloys Compd* 261:273
266. Chartouni D, Zuttel A, Nutzenadel C, Schlapbach L (1997) *J Alloys Compd* 260:265
267. De Vidts P, Delgado J, White RE (1995) *J Electrochem Soc* 142:4006
268. Chirkov YuG, Pshenicnikov AG (1990) *Elektrohimiya* 26:864
269. Viitanen M (1993) *J Electrochem Soc* 140:936
270. Heikonen J, Nojonen T, Lampinen M (1996) *J Power Sources* 62:27
271. Heikonen J, Vuorilehto K, Nojonen T (1996) *J Electrochem Soc* 143:3972
272. Heikonen J (1997) *J Power Sources* 66:61
273. Paxton B, Newman J (1997) *J Electrochem Soc* 144:3818
274. Gu WB, Wang CY (1998) *J Electrochem Soc* 145:3418
275. Yang T-H, Pyun S-I (1998) *Electrochim Acta* 43:471
276. Yang QM, Ciureanu M, Ryanm DH, Ström-Olsen (1994) *J Electrochem Soc* 141:2108
277. Ciureanu M, Yang QM, Ryan DH, Ström-Olsen (1994) *J Electrochem Soc* 141:2430
278. Meli F, Züttel A, Schlapbach L (1994) *Z Phys Chem NF* 183:371
279. Iwakura C, Oura T, Inoue H, Matsuoka M (1996) *Electrochim Acta* 41:117
280. Kim DM, Lee SM, Jung JH, Jang KJ, Lee JY (1998) *J Electrochem Soc* 145:93
281. Peng W, Redey L, Jansen AN, Vissers DR, Myles KM, Carpenter JM, Richardson JW, Burr GL, Selman JR (1997) *J Electrochem Soc* 144:3836
282. Kim DM, Lee SM, Jang KJ, Lee JY (1998) *J Alloys Compd* 268:241
283. Lee HH, Lee KY, Lee JY (1997) *J Alloys Compd* 260:201
284. Züttel A, Schlapbach L, Cartouni D, Meli F (1995) Report on IV international conference on hydrogen materials science and chemistry of metal hydrides. Katsiveli, Crimea, Ukraine
285. Nakamura Y, Sato K, Fujitani S, Nishio K, Oguro K, Uehara I (1998) *J Alloys Compd* 267:205
286. Kim JW, Lee SM, Lee HI, Kim DM, Lee JY (1997) *J Alloys Compd* 255:248
287. Inoue H, Araiand S, Iwakura C (1996) *Electrochim Acta* 41:937
288. Iwakura C, Kasuga H, Kim I, Inoue H, Matsuoka M (1996) *Electrochim Acta* 41:2691
289. Iwakura C, Hazui S, Inoue H (1996) *Electrochim Acta* 41:471
290. Bernard P (1998) *J Electrochem Soc* 145:456
291. Leblanc P, Jordy C, Knosp B, Blanchard P (1998) *J Electrochem Soc* 145:860
292. Zhou Z, Yan J, Li Y, Song D, Zhang Y (1998) *J Power Sources* 72:236
293. Leblanc P, Blanchard P, Senyarich S (1998) *J Electrochem Soc* 145:844
294. Ikoma M, Yuasa S, Yuasa K, Kaida S, Matsumoto I, Iwakura C (1998) *J Alloys Compd* 267:252
295. Zhu WHH, Zhang GD, Zhang DJ, Ke JJ (1997) *J Chem Technol Biotechnol* 69:121
296. Mukerjee S, Mcbreen J, Adzic G, Johnson JR, Reilly JJ, Marrero MR, Soriaga MP, Alexander MS, Visintin A (1997) *J Electrochem Soc* 144:L258
297. Chen J, Dou SX, Bradhurst D, Liu HK (1998) *J Power Sources* 70:110
298. Jang KJ, Jung JH, Kim DM, Yu JS, Lee JY (1998) *J Alloys Compd* 268:290